Precambrian Research 182 (2010) 351–372

Contents lists available at ScienceDirect

Precambrian Research

journal homepage: www.elsevier.com/locate/precamres

C-, Sr-isotope and Hg chemostratigraphy of Neoproterozoic cap carbonates of the Sergipano Belt, Northeastern Brazil

Alcides Nobrega Sial[a,*], Claudio Gaucher[b], Marinho Alves da Silva Filho[c], Valderez P. Ferreira[a], Marcio M. Pimentel[d], Luiz D. Lacerda[e], Emmanoel V. Silva Filho[f], Wilker Cezario[a]

[a] NEG-LABISE, Department of Geology, UFPE, C.P. 7852, Recife, 50670-000, Brazil
[b] Department Geología, Facultad de Ciencias, Iguá 4225, 11400 Montevideo, Uruguay
[c] Companhia de Pesquisa de Recursos Minerais – CPRM, Recife, Brazil
[d] Institute of Geosciences, University of Brasilia, Brasilia, 70910-900, Brasília-DF, Brazil
[e] Labomar, Federal University of Ceará, Fortaleza, Ceará, Brazil
[f] Department of Geochemistry, Federal Fluminense University, Niteroi, R.J., 24020-007, Brazil

ARTICLE INFO

Article history:
Received 11 June 2009
Received in revised form
19 November 2009
Accepted 5 May 2010

Keywords:
Neoproterozoic
Cap carbonate
Snowball Earth
Chemostratigraphy
Northeastern Brazil

ABSTRACT

Two cap carbonates overlying glaciogenic diamictites crop out extensively in the eastern Vaza Barris Domain of the Sergipano Belt, northeastern Brazil. They are represented by carbonates of the Jacoca Formation, resting on top of diamictite of the Ribeiropolis Formation, and by the Olhos D'Agua Formation (carbonates, organic-rich towards the top), which overlies diamictite of the Palestina Formation. These two sequences were deformed and metamorphosed at sub-greenschist facies-conditions during the Brasiliano cycle (650–600 Ma).

In the western Vaza Barris Domain, dolostone of the Acauã Formation rest, in sharp contact, on diamictites of the Juetê Formation and are much less deformed than the Olhos D'Agua Formation.

Values of (^{13}C for the Jacoca and Acauã Formations cluster around −4 to −5‰. In the Olhos D'Agua Formation, however, negative values (around −5‰) in the shallow-marine base of the sequence are replaced up section by values close to zero and, abruptly, by positive values between +8 and +10‰ at the top. Strontium-isotope ratios for carbonates of these three formations are within the range of late Neoproterozoic seawater (0.7060–0.7090). The Acauã Formation displays $^{87}Sr/^{86}Sr$ ratios from 0.7072 to 0.7073, while the Jacoca and Olhos D'Agua formations display values within the range from 0.7077 to 0.7081. Strontium-isotopes coupled with available C-isotopes, detrital zircon U–Pb ages and structural data suggest that the Jacoca Formation and Acauã are probably correlative and mid Cryogenian in age, and that the Olhos D'Agua Formation is lowermost Ediacaran (Marinoan) in age.

Mercury concentrations in carbonates of the Jacoca, Olhos D'Agua and Acauã formations are usually much higher than those observed in carbonates deposited not concomitantly with volcanic activities (<3 ng g^{-1}). They are, in fact, similar to those in carbonates deposited during volcanic activity (e.g. Tertiary Punta Rocallosa carbonates in Chile), with concentration values between 20 and 80 ng g^{-1}, suggesting that CO_2 in the basal portion of these carbonate formations is mostly mantle-derived, accumulated in the atmosphere during Cryogenian-Ediacaran glacial events.

Published by Elsevier B.V.

1. Introduction

The Sergipano Belt is a Neoproterozoic fold-and-thrust belt located in the northeastern margin of the São Francisco Craton (Fig. 1). It was formed by continental collision between the Congo-São Francisco Craton and the Pernambuco-Alagoas Massif during the Brasiliano/Pan-African orogeny (Brito Neves et al., 1977). From a geodynamic perspective, it has been interpreted as a collage of lithostratigraphic domains (Davison and Santos, 1989; Silva Filho, 1998) or as a Neoproterozoic fold-and-thrust belt produced by inversion of a passive margin basin located at the northeastern margin of the São Francisco plate (D'el Rey Silva, 1999).

This belt consists, from north to south, of six lithostratigraphic domains (Figs. 2–4) separated from each other by major shear zones: Canindé, Poço Redondo, Marancó, Macururé, Vaza Barris and Estância (Santos and Souza, 1988; Davison and Santos, 1989; Silva Filho, 1998). The Macururé, Vaza Barris and Estância domains are composed mostly of metasedimentary rocks with metamorphic grade from weak (or non-metamorphic in the Estância Domain)

* Corresponding author. Tel.: +55 81 2126 8242; fax: +55 81 2126 8242.
E-mail address: sial@ufpe.br (A.N. Sial).

0301-9268/$ – see front matter. Published by Elsevier B.V.
doi:10.1016/j.precamres.2010.05.008

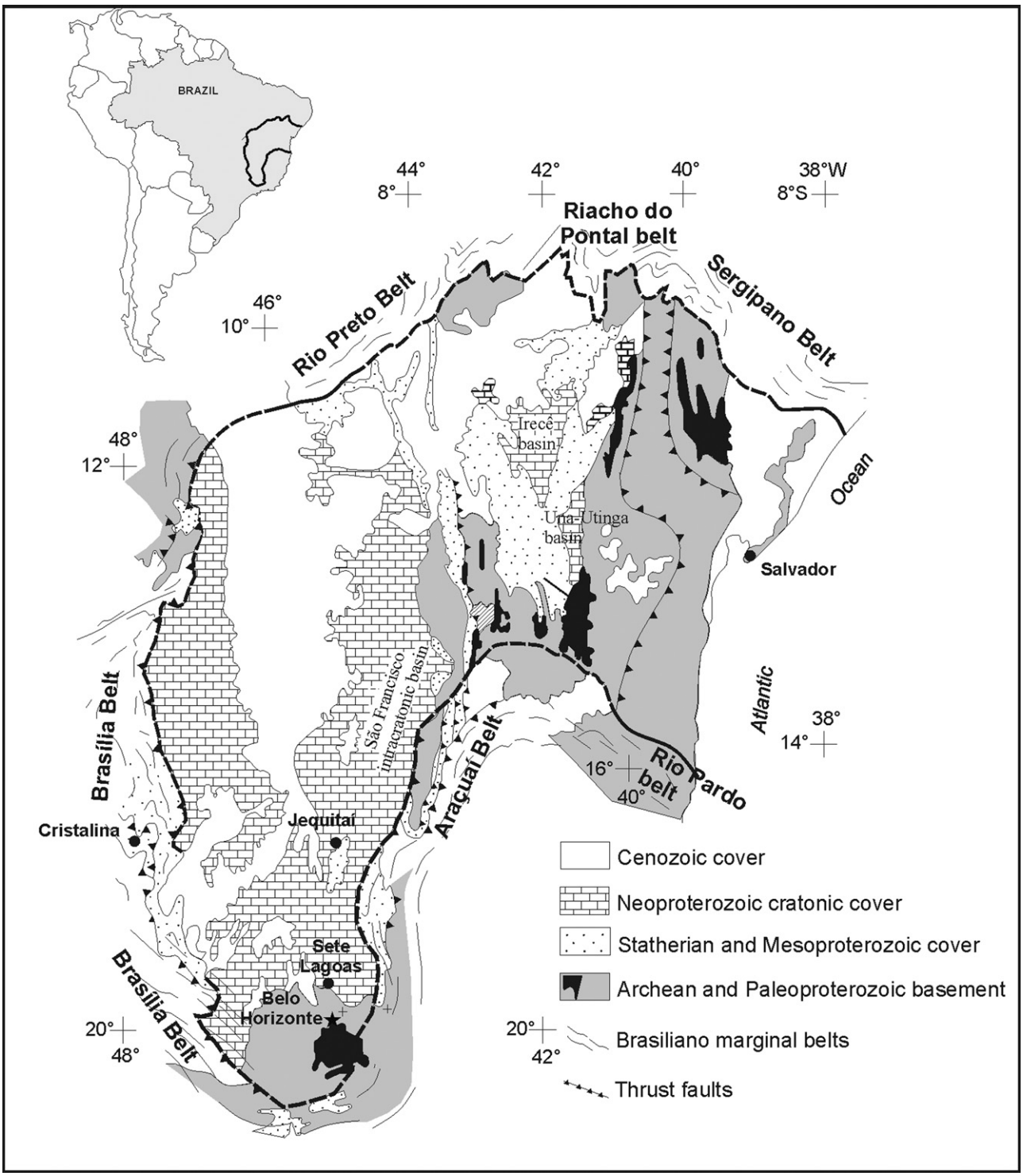

Fig. 1. Simplified geological map of the São Francisco craton showing the Neoproterozoic cover and surrounding belts (Sial et al., 2010).

through greenschist facies in the Vaza Barris domain to amphibolite facies in the Macururé Domain. Silva Filho and Torres (2002) and Silva Filho et al. (2003) have proposed three additional domains: Rio Coruripe,Viçosa and Pernambuco-Alagoas. Further geological details on all domains of the Sergipano Belt are found in Davison and Santos (1989) and Santos et al. (1998).

Neoproterozoic diamictite-carbonate couplets occur in the Vaza Barris and Estância domains, namely: Juetê-Acauã, Ribeirópolis-Jacoca and Palestina-Olhos D'Agua formations, which have been regarded as Neoproterozoic cap carbonates by Sial et al. (2000, 2006, 2010). At least two different diamictite horizons occur in several sections, which, along with the excellent exposures in a semi-desert area, make them prime targets for the investigation of the profound environmental oscillations associated to Neoproterozoic glaciations.

So far, at least four distinct Neoproterozoic glacial events were recognized, the oldest being the Kaigas-Chuos glacial event around 745 Ma (Frimmel et al., 1996; Hoffman et al., 1996). The mid-Cryogenian glaciation usually referred to as "Sturtian" likely represents at least two different glacial events at ca. 710 and 660

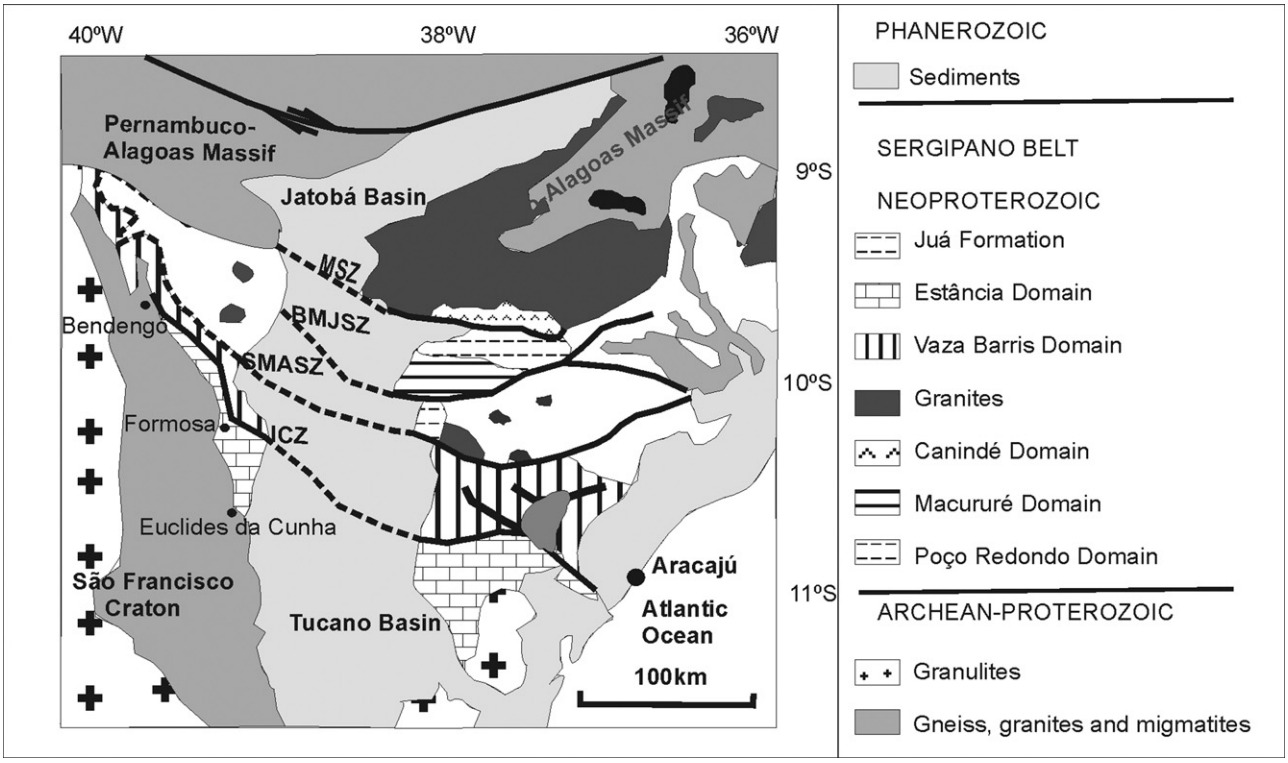

Fig. 2. Domains of the Sergipano belt (modified from D'el Rey Silva, 1995). MSZ, BMJSZ, SMASZ and ISZ represent, respectively, the Macururé, Belo Monte-Jeremoabo, São Miguel do Aleixo and Itaporanga shear zones.

Ma (Fanning and Link, 2004; Xu et al., 2009; Hoffman and Li, 2009, and references therein), the latter being the age of the type Sturtian glacials in Australia (Fanning, 2006). The most severe glacial event marks the end of the Cryogenian ("Marinoan" glaciation), and ended at around 635 Ma (Hoffmann et al., 2004; Condon et al., 2005). The mid-Ediacaran Gaskiers glacial event, tightly constrained between 583.7 ± 0.5 and 582.1 ± 0.5 Ma (Bowring et al., 2003), is often cited as the youngest Neoproterozoic glaciation (i.e. Hoffman and Li, 2009). However, there is growing evidence for at least one late Ediacaran (ca. 547 Ma), Phanerozoic-type glaciation well represented in SW-Gondwana (Vingerbreek glacial event: Germs, 1995; Germs et al., 2009 and references therein) and in Central Asia (Baykonurian Glaciation: Chumakov, 2009 and references therein).

Carbon- and strontium-isotope chemostratigraphy have become established tools for the study of the relative chronology of glacial events and its ubiquitous cap carbonates (e.g. Jacobsen and Kaufman, 1999; Halverson et al., 2005, 2007, 2009; Kaufman et al., 1993, 2009). Moreover, it has been shown that Neoproterozoic glaciations were accompanied or even caused by severe perturbations of the carbon cycle (e.g. Kaufman et al., 1997), which makes carbon isotope chemostratigraphy a very important tool for unraveling the causes of the glacial events and their impact on the biosphere.

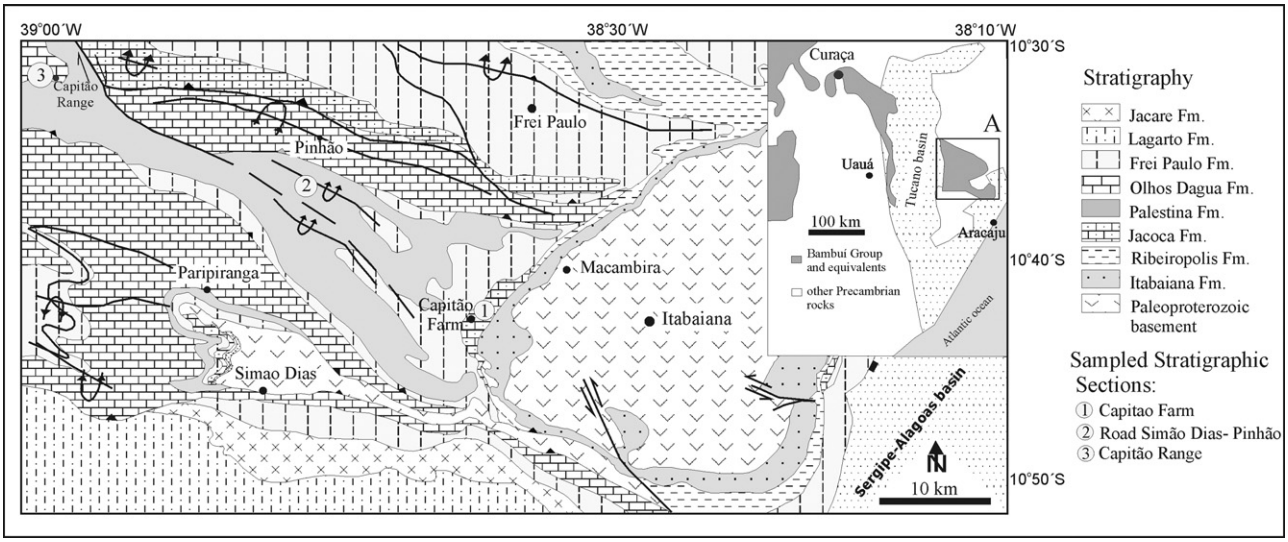

Fig. 3. Simplified geological map of the eastern Vaza Barris Domain, Sergipano Belt (modified from D'el Rey Silva, 1999), with the indication of sampled stratigraphic sections in the present study.

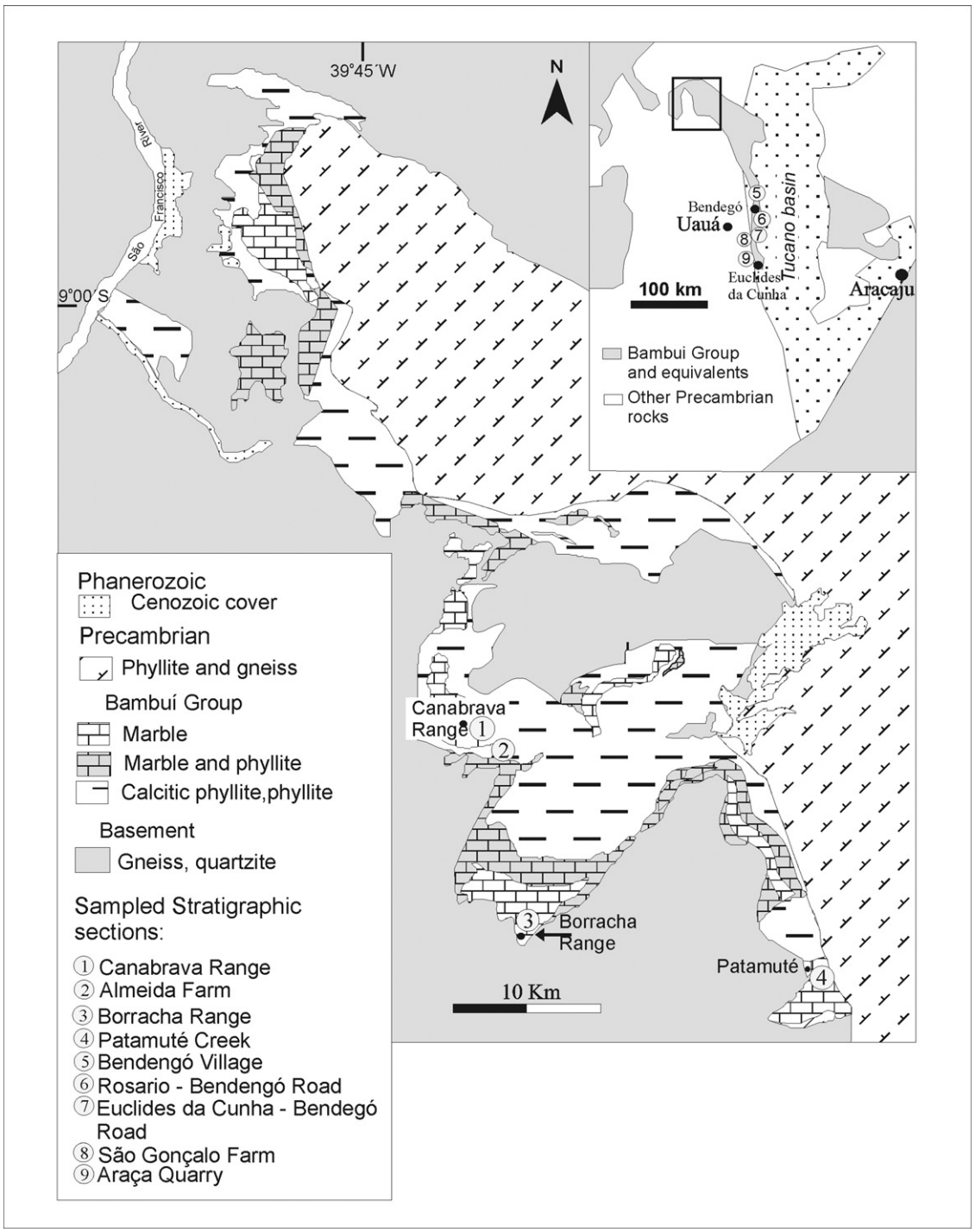

Fig. 4. Simplified geological map of the western Vaza Barris Domain, Sergipano Belt (modified from Jordan, 1973), with the indication of sampled stratigraphic sections in the present study.

We report in this study the results of a chemostratigraphic survey (C, Sr) of the Neoproterozoic, diamictite-bearing sedimentary successions of the Sergipano Belt, aiming at constraining their relative chronology and correlation with similar units in southwestern Gondwana. Additionaly, a preliminary discussion on the use of mercury chemostratigraphy of post-glacial cap carbonates as a proxy of volcanic activity in the aftermath of extreme glacial events is presented.

2. Geologic setting, stratigraphy and age

2.1. Geologic setting and stratigraphy

The structure and lithology of the Sergipano Belt have been compared to the Ndjolé Series of northern Gabon in Africa (Allard and Hurst, 1969). Later, it has been compared with sequences of Mbalmayo-Bengbis, Dja, and Sembe Ouesso of southern Cameroon

	Group	Formation	Group	Formation	Group	Formation	Lithology and thickness	Group	Formation
	Humphrey and Allard (1969)		Silva Filho and Brito Neves (1979)		D´el-Rey Silva (1995)		D´el-Rey Silva (1995), Davison and Santos (1989)	This study	
Neoproterozoic	Vaza Barris	Frei Paulo/ Ribeiropolis	Estancia	Lagarto	Vaza Barris	Olhos D´Água	Interbedded limestone and shales, mainly deposited below wave base (200-1300m)	Simão Dias	Jacaré Lagarto-Palmares (<565Ma)
						Palestina	Polimict diamictite, poorly sorted, pelitic matrix (100-500m)		
		Olhos D´Água		**Acauã**	Simão Dias	Frei Paulo	Silty phyllite, metasandstone and wacke (100-500m)	Vaza Barris	Frei Paulo/Ribeiropolis (<620 Ma)
						Jacaré	Metasiltite, medium-grained metasandstone (50-200m)		Olhos DÁgua
						Lagarto-Palmares	Coarse-upwarding sequence of mudstone,siltstone, Sandstone, and lithic wacke (50-300		Capitão/Palestina (<653 Ma)
	Miaba	Capitão/Palestina			Miaba	Jacoca	Grey limestones and dolostones with intercalated gray shales (0-300m)	Miaba	Jacoca/ Acauã
		Jacoca / Jacarecica				Ribeirópolis	Metagreywacke, pebbly phyllite, argillite and diamictite (0-500m)		**Ribeirópolis/Juetê** /Jacarecica (<780Ma)
		Itabaiana		**Juetê**		Itabaiana	Massive shallow marine and fluvial quartzites (10-700m)		Itabaiana
	Basal unconformity								
Paleoproterozoic to Archean basement gneisses									

Fig. 5. Summary stratigraphic chart for the Miaba and Vaza Barris and Estancia groups, Sergipano Belt (compiled from Humphrey and Allard, 1969; Silva Filho and Brito Neves, 1979; D'el Rey Silva, 1995; Davison and Santos, 1989).

and northern Congo (Cordani, 1973). According to Trompette (1994), this belt represents the Brazilian counterpart of the Oubanguides and, together, they form a roughly E–W elongated mega-orogen more than 5000 km long. More recently, the Sergipano Belt has been correlated with the Yaoundé Belt (Cameroon, Africa) by Oliveira et al. (2006).

Stratigraphic studies on the Vaza Barris and Estancia domains of the Sergipano Belt, were pioneered by Humphrey and Allard (1969) who divided the supracrustal sequences into two groups, Miaba and Vaza Barris. Their stratigraphic scheme has been later modified by Silva Filho (1998), Silva Filho and Brito Neves (1979) and D'el Rey Silva (1995, 1999) as shown in Fig. 5. Among the most relevant modifications, D'el Rey Silva (1995, 1999) proposed that the Ribeiropolis Formation is older than formerly believed, placing it below the Jacoca Formation. It is assumed here that the Frei Paulo Formation rests on top of the Olhos D'Agua Formation as accepted by most authors (Humphrey and Allard, 1969; Silva Filho, 1998; Silva Filho and Brito Neves, 1979; Davison and Santos, 1989).

The Estancia Group in northern Bahia, according to Silva Filho and Brito Neves (1979), comprises the Juetê, Acauã and Lagarto formations. These authors hypothesized that the Juetê and Ribeiropolis formations could be correlative as well as the Acauã and Jacoca formations, a contention that needs further investigation.

Two depositional cycles both represented by a basal continental to shallow-marine siliciclastic succession, overlain by a carbonate sequence, have been recognized by D'el Rey Silva (1995, 1999). These two cycles, with slight modifications, are:

(a) Cycle I (Estancia-Miaba Group) with a siliciclastic succession including the Itabaiana (conglomerate, quartzite, metasiltite), Juetê (sandstone, diamictite) and Ribeiropolis (silty phyllite, metagreywacke, pebbly phyllite, diamictite) formations, overlain by a carbonate succession, represented by the Jacoca Formation, stratigraphically equivalent to the Acauã Formation;

(b) Cycle II represented by a siliciclastic succession (Lagarto-Palmares and Jacaré formations of the Simão Dias Group) overlain by the Vaza Barris Group. The latter comprises diamictite of the Palestina Formation overlain by carbonates of the Olhos D'Agua Formation, and pelites and subordinate carbonates of the Frei Paulo Formation. These two successions underwent sub-greenschist facies metamorphism which preserved original sedimentary structures.

The Estancia-Miaba Group is well exposed around the Itabaiana and Simão Dias basement domes in Sergipe (Fig. 3). The Ribeiropolis Formation is 0–300 m thick around the Itabaiana dome and locally reaches a thickness of about 500 m within the belt. It consists of diamictite, metagreywacke and quartz-sericite phyllite transitionally overlying quartzite of the Itabaiana Formation. The occurrence of volcanic rocks in this formation, the west of the Simão Dias dome, has been reported by D'el Rey Silva (1995, 1999). Carbonates of the Jacoca Formation are seen in sharp contact on top of the Ribeiropolis diamictite (Fig. 6a, b) at the Capitão Farm along the Salgado River (western side of the Itabaiana dome). A typical section of the Jacoca Formation starts with a thick layer of laminated gray to pink dolostone containing possibly primary stratabound pyrite and chalcopyrite. This is followed upsection by a 3–15 m thick layer of laminated dolostone, and dark gray to black phyllite and about 10 m thick bed of massive dolostone. This unit is overlain by a 40 m thick heterolithic sequence of gray limestone and dark to black phyllite and finally by gray dolostone.

At the Capitão Farm, the cap dolostone shows wavy lower contact. Clasts at the top of the diamictite of the Ribeiropolis Formation are concentrated and salient (Fig. 6b) as a result, perhaps, of lithification and erosion prior to cap dolostone deposition. Features suggesting soft sediment deformation were observed in the diamictites and cap carbonates (Fig. 7a), which may be interpreted as the result of a rapid icehouse to greenhouse transition (e.g. Puga cap carbonate, Amazon craton; Nogueira et al., 2003). Well-developed tubestone stromatolites occur in the dolostone cap carbonate in the Capitão Farm (Fig. 7b and c).

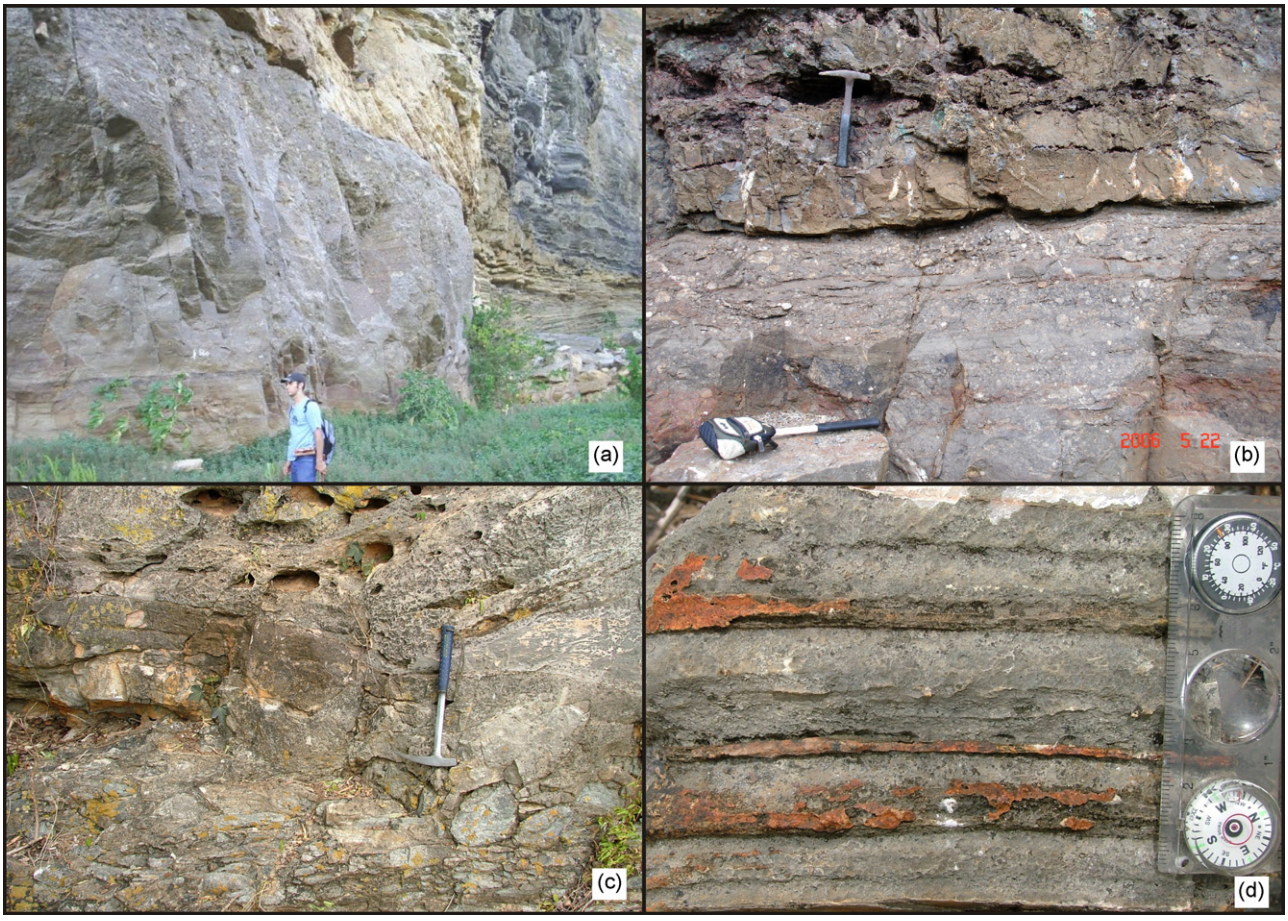

Fig. 6. (a) Two meter-thick dolostone bed of the Jacoca Formation in sharp contact with diamictite of the Ribeiropolis Formation and overlain, in turn, by a sequence of marls and pelite in a zebra-like pattern (Capitão Farm, Sergipe); (b) diamictite of the Ribeiropolis Formation in knife-sharp contact with dolostones of the Jacoca Formation, Capitão Farm, Sergipe. Dolostone shows wavy contact and some bedding is observed in the diamictite. Some clasts at the top of the diamictite are concentrated and salient (lithification and erosion prior to dolostone deposition?); (c) contact between cap dolostone of the Acauã Formation and diamictite of the Juetê Formation, at the Serra da Borracha range, about 20 km west of Patamuté, Bahia; (d) micritic calcitic limestone with intercalation of thin dolostone beds (rhythmite) with parallel lamination. Dolostone layers are locally boudinated, Serra da Borracha, Bahia.

Carbonates of the Acauã Formation overlie either the Juetê Formation diamictite or rest unconformably on basement gneiss. Well-preserved exposures of this contact occur in the western Vaza Barris Domain, between Euclides da Cunha and Bendegó villages, at Patamuté village and at the Serra da Borracha and at Serra da Canabrava (northeastern Bahia). The type locality of the Juetê Formation is at the Juetê River, about 6 km south of Bendegó, where it shows total thickness of about 30 m and is composed of buff sandstone, diamictite (about 15 m thick) and reddish feldspathic sandstone and reddish claystone (Silva Filho and Brito Neves, 1979). Diamictite of the Juetê Formation contains clasts of granite, orthogneiss, phyllite or quartzite up to 0.6 m in diameter, and locally display Fe-rich shale beds at the base. At São Gonçalo Farm dropstones with vertical axes ("bullet-clasts") occur in the upper, stratified portion of the diamictite. Possible striated clasts and "dreikanters" were also observed.

The Acauã Formation consists of a thin cap dolostone showing hummocky and, locally, pseudo-tepee structures (Fig. 8a). It is overlain by a fining- and thinning-upward (transgressive) carbonate succession comprising limestone and limestone/dolostone or limestone/shale rhythmites (Fig. 8b and c). Continuous sections of the Acauã Formation are exposed at Serra da Borracha and at Serra da Canabrava, as well as Patamuté Creek at Patamuté village and São Gonçalo Farm, about 25 km to the north of Euclides da Cunha village (Bahia). In proximal sections, such as the Serra da Borracha (20 km west of Patamuté, Bahia), limestone immediately on top of the cap dolostone often bear outsized clasts up to 2 m across (Fig. 9a and b). The clasts are exclusively made up of dolostone, and clearly pierce and deform underlying laminations. Similar dolostone clasts in a carbonate matrix occur in the glaciogenic Ghaub Formation in Namibia and have been interpreted as dropstones (Hoffman et al., 1998; Hoffmann et al., 2004). However, in the case of the Acauã Formation this interpretation is not straightforward, because slumped beds 1–2 m in thickness occur at the same level. They are characterized by E-verging (basinwards) convolute bedding and basal detachment surfaces, thus showing that the outsized clasts may represent dismembered dolostone beds. High sedimentation rates and/or glaciotectonic instability may thus account for both the slumps and lonestones.

The Olhos D'Agua Formation (200–1300 m) is composed of interbedded limestones (organic-rich towards the top) and green, calcareous chlorite-schist and silty phyllite. It overlies diamictite and pebbly metagreywacke of the Palestina Formation (Fig. 10 a, b, and c). Marble beds are interbedded with blue to black, fine-grained metalimestone and gray metadolostone. The thick carbonates around the Simão Dias dome (Fig. 3) pass upward into supratidal-intertidal facies with oolites and wave-reworked sedimentary structures indicating a near-shore environment (D'el Rey Silva, 1995). At the Capitão Range, about 25 km northwest of Paripiranga, Bahia, a 10 m thick dolostone layer of the Olhos D'Agua Formation is in sharp contact with diamictite of the Palestina Formation (metagreywacke with clasts up to 30 cm in diameter) and

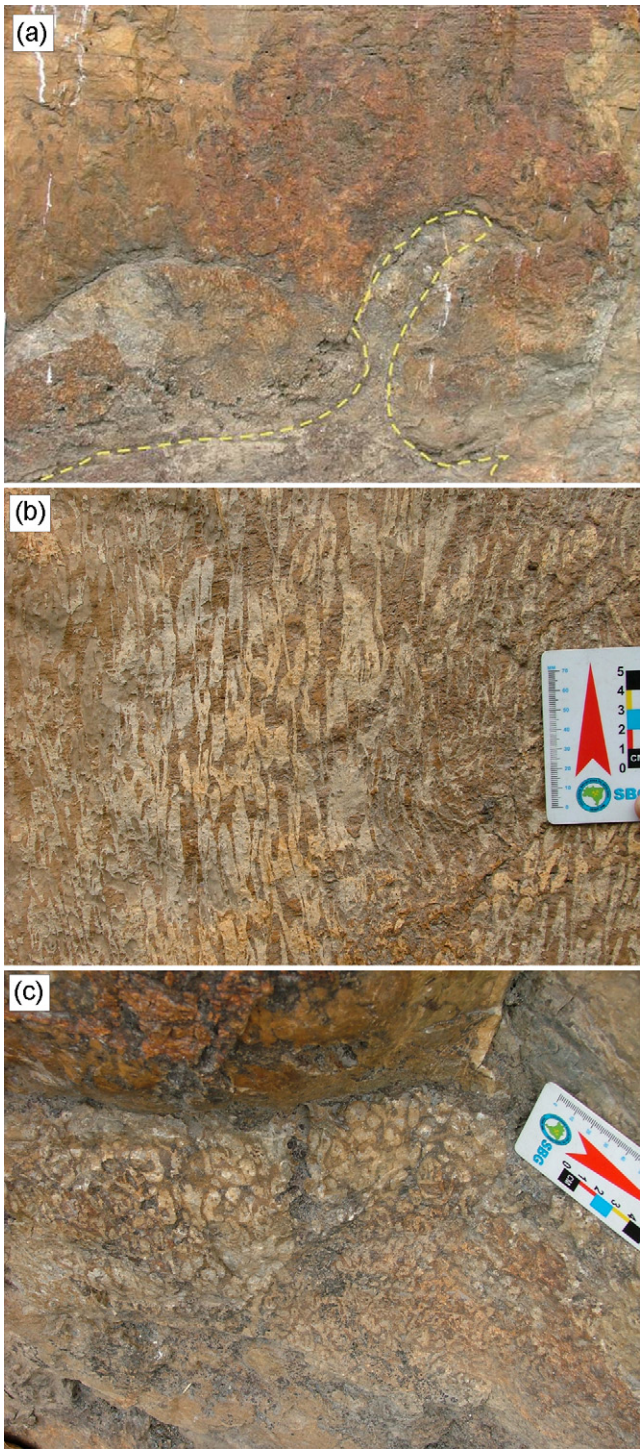

Fig. 7. (a) Contact between Jacoca Formation biostroma in a cap dolostone and underlying diamictite of Ribeirópolis Formation suggesting soft sediment-deformation from abrupt change from icehouse to greenhouse; (b) plan of view of tubestone stromatolite in the cap carbonate of Jacoca Formation at Capitão Farm; (c) tubestone stromatolites in longitudinal section.

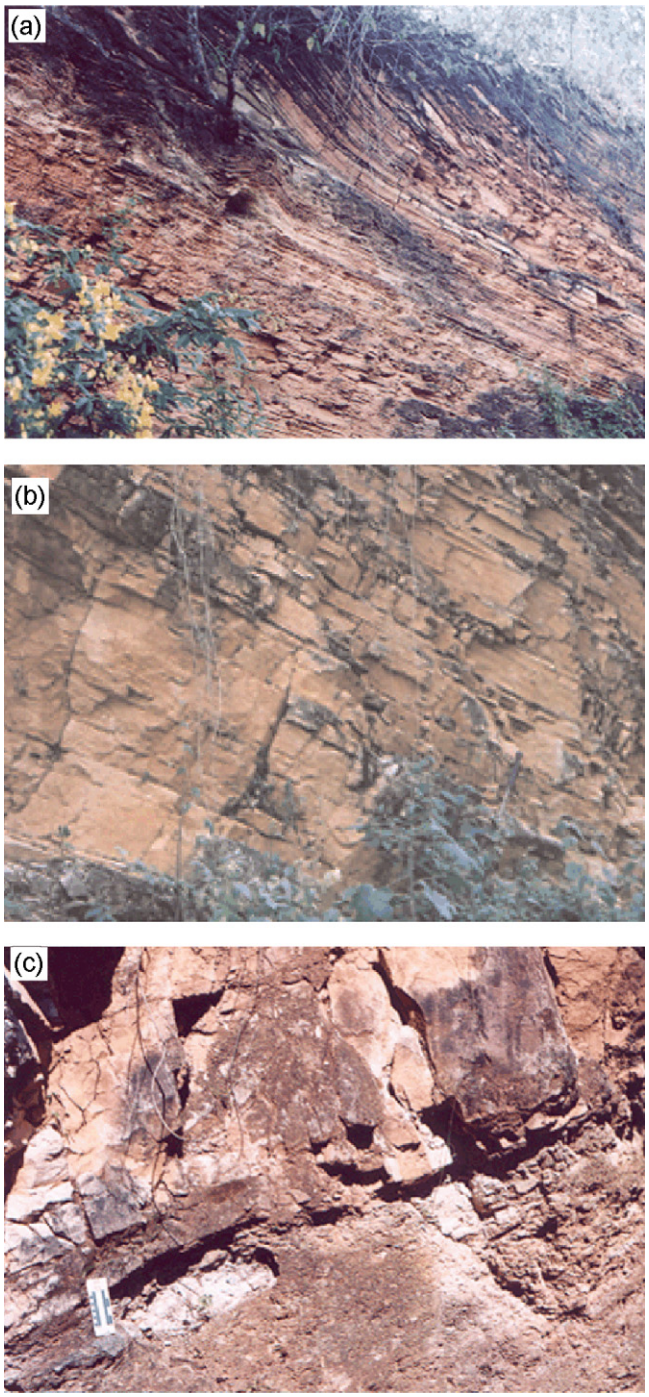

Fig. 8. (a) Juetê Formation diamictites overlain by Acauã Formation dolostones with hummocky and cross-stratification at the São Gonçalo Farm, north of Euclides da Cunha village; (b) and (c) post-glacial fining- and thining-upward sequence (thus deepening-upward sequence).

followed up section by about 50 m of limestone-pelite intercalations. They are in turn overlain by laminated limestone (40 m thick) culminating with a 30 m thick layer of organic-rich black limestone.

2.2. Geochronology

Geochronological data for the Sergipano Belt reported by Oliveira et al. (2006), Oliveira (2008) indicate that clastic and chemical sedimentary rocks of the Vaza Barris Domain rest on Archean basement dated at 2868 ± 25 Ma (U–Pb SHRIMP zircon age, Simão Dias dome, Sergipe). Detrital zircon grains from the Itabaiana Formation quartzite have yielded ages older than 2000 Ma whereas metasandstone of the Ribeiropolis Formation exhibits two zircon age populations, one around 2000 Ma and, a subordinate one, at 780 Ma according to the same authors. The youngest detrital zircon grains from the Palestina diamictite are 653 Ma (Oliveira, 2008) and from the Frei Paulo Formation are 620 Ma old (Oliveira et al., 2006; Oliveira, 2008) and suggest the Borborema Province, further north,

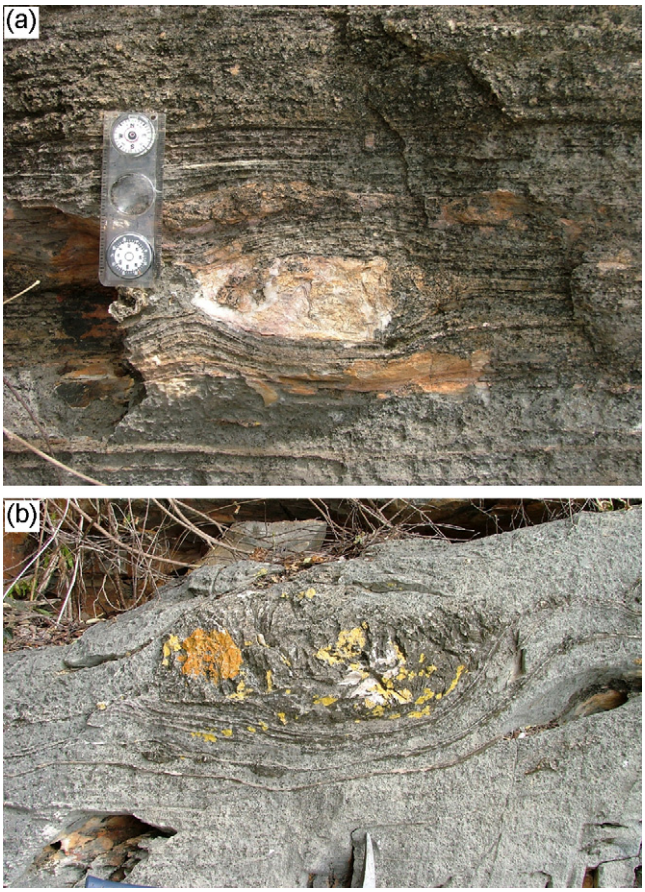

Fig. 9. (a and b) Dolostone lonestone in limestones at the Serra da Borracha range, Bahia.

as the likely source area of these sediments. Rocks of the Miaba and Vaza Barris groups have been metamorphosed and deformed in the Brasiliano cycle at 628 ± 12 Ma (Oliveira et al., 2006).

In the present study, we carried out a provenance study of the Ribeiropolis Formation (Capitão Farm, Sergipe) using LA-ICPMS U–Pb ages of detrital zircons. Ages cluster around 2900 and 2100 Ma, with subordinate peaks around 2500, 1500 and 1000 Ma (Fig. 11).

Zircon grains from a supposedly metavolcanic rock from the Riachinho Farm, 7 km north of the Ribeiropolis village have been analyzed in Australia (U–Pb, SHRIMP) by R.V. Van Schmus in an attempt to date the deposition of this sequence (written communication, 2009). Unfortunately, nearly all the zircon grains are Paleoproterozoic, with only two presenting Neoproterozoic ages of 850 and 810 Ma, and those could also be detrital.

In summary, the current geochronological data indicate that the deposition of Jacoca Formation carbonates is younger than 780 Ma and the deposition of the Olhos D'Agua Formation carbonates took place after 653 Ma and before 628 Ma.

Detrital zircon grains from the diamictite of the Juetê Formation, to the north of Euclides da Cunha, are older than 2073 Ma (Oliveira, 2008) and detrital zircon grains from sandstones of the Lagarto (on top of the Acauã Formation) and Palmares formations display ages that cluster around 565 Ma, 582, 633 Ma, 956 Ma, 977 Ma and 1855 Ma.

2.3. Chemical and isotope stratigraphies

The sections investigated here show well-preserved cap carbonates in knife-sharp contact with basal diamictites as known for Neoproterozoic cap carbonates worldwide (e.g. Kennedy, 1996; Hoffman and Schrag, 2002).

Several localities in the eastern and western Vaza Barris domains exhibit this feature. Among them, we have chosen and stratigraphically sampled carbonates of the Jacoca Formation in sharp contact with diamictite of the Ribeiropolis Formation at Capitão Farm (Fig. 6a). The Acauã Formation overlies with sharp contact diamictites of the Juetê Formation at the Serra da Borracha range (Fig. 6c), at the Patamuté Creek in the Patamuté village as well as at São Gonçalo Farm in the state of Bahia (Fig. 8). Besides, carbonates of the Olhos D'Agua Formation in sharp contact with diamictite of thePalestina Formation, at the Capitão Range, were also sampled.

Several other localities in Sergipe and Bahia offer exposures of carbonate rocks of the Jacoca, Acauã and Olhos D'Agua formations that can help understanding the geological and paleoclimatic evolution of the Vaza Barris Domain. Among them, we sampled well-preserved carbonate exposures of the Acauã Formation at the Serra da Canabrava and at the Almeida Farm near the Serra da Borracha, and along the road between Euclides da Cunha and Bendengó (Bahia). Besides, continuous outcrops of the Olhos D'Agua Formation in the road Rosario-Cocorobó, Bahia, and south of Pinhão village, Sergipe, were also sampled.

2.3.1. Sample selection and preparation

Samples were collected along traverses, perpendicular to the strike of the carbonate strata, at meter intervals. Analyses of C and O isotopes of carbonates were performed at the stable isotope laboratory (LABISE), Federal University of Pernambuco, Brazil. For the Sr isotopes, samples have been chemically treated at the LABISE and sent to Brasilia for isotope ratio analyses. Analyses of Hg were partially performed at the Instituto de Ciencias do Mar (Labomar), Fortaleza, Ceará and partially at the Department of Geochemistry, Federal Fluminense University, Niteroi, Brazil.

2.3.2. Analytical methods

Only least altered portions of samples were micro-drilled with a 1 mm drill bit. CO_2 was extracted from these carbonate samples on a high vacuum line after reaction with phosphoric acid at 25 °C, and cryogenically cleaned, according to the method described by Craig (1957). Released CO_2 gas was analyzed for O and C isotopes in a double inlet, triple collector mass spectrometer (VG Isotech SIRA II), using the BSC reference gas (Borborema skarn calcite) that was calibrated against NBS-18, NBS-19 and NBS-20, and has the (^{18}O value of −11.3‰ PDB and ($^{13}C = 8.6‰ PDB. The external precision based on multiple standard measurements of NBS-19 was better than 0.1‰ for carbon and oxygen. Isotope analyses are expressed in the (-notation in parts per thousand in relation to the international PDB standard. Selected samples were also analyzed for major and trace elements at the LABISE, by X-ray fluorescence, using fused beads and an automatic RIX-3000 (RIGAKU) unit. Fused beads were prepared using Li fluoride and Li tetraborate and uncertainties were better than 5% for Sr and Fe and 10% for Mn.

For determination of the Sr isotopic ratios, powdered samples were leached in 0.5 M acetic acid and centrifuged to separate the soluble from the insoluble fractions. Strontium was eluted from solutions by ion exchange chromatography using Sr-Spec resin. $^{87}Sr/^{86}Sr$ values were determined in static mode using a Finnigan MAT 262 seven-collector mass spectrometer at the University of Brasília, Brazil. The isotopic ratios were normalized to $^{86}Sr/^{88}Sr$ value of 0.1194 and the 2σ uncertainties on Sr-isotope measurements was less than 0.00009. Repeated analyses of NBS 987 standard indicated the value of 0.71024 ± 0.00007 (2σ) for the $^{87}Sr/^{86}Sr$ ratio.

For determination of total Hg concentrations, homogenized 0.5–1.0 g samples of sediments, dried at 60 °C to constant weight, were digested with an acid mixture (50% *acqua regia* solution), and

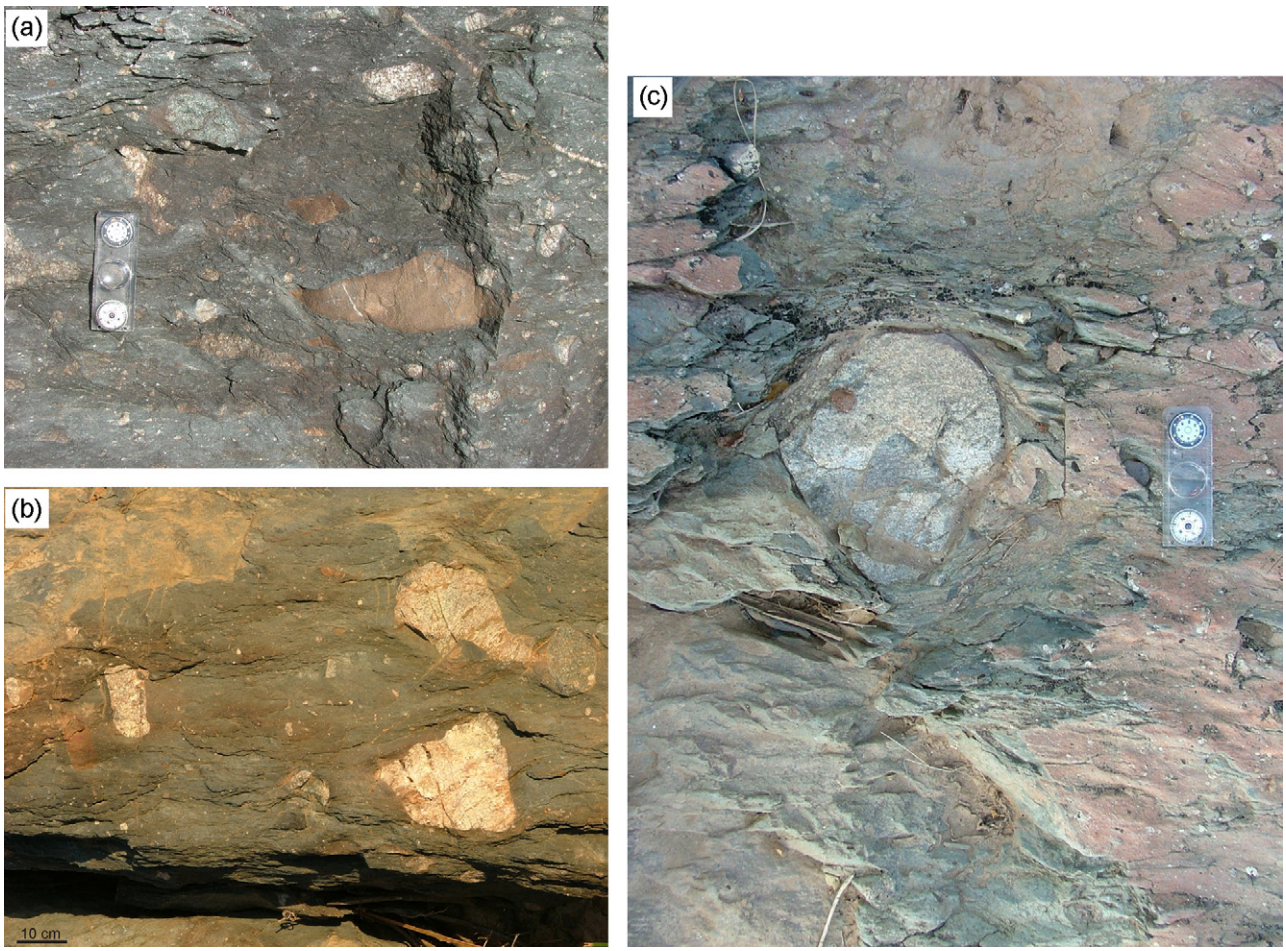

Fig. 10. (a) Diamictite (metagreywacke matrix) of the Palestina Formation with some carbonate clasts of Jacoca Formation, at the road Simão Dias-Pinhão, state of Sergipe; (b) Granitic clasts and (c) bullet clast in diamictite of the Palestina Formation, Capitão Range, near Paripiranga, Bahia. Width of picture = 60 cm.

heated at 70 °C for 1 h, in a thermal-kinetic reactor "cold finger". Glass and plastic ware were decontaminated by immersion for 2 days in 10% (v/v) Extran solution (MERCK), followed by immersion for 3 days in diluted HNO_3 (10% v/v) and final rinsing with Milli-Q water. All chemical reagents used were of at least analytical grade. Cold Vapor Atomic Absorption Spectrophotometry, using a Bacharach Coleman (50D model) equipment, was used for Hg determination, after Hg^{2+} reduction with $SnCl_2$. All samples were analyzed in duplicates, showing reproducibility within 9.5%. A certified reference material (NRC PACS-2, Canada) was simultaneously analyzed to evaluate Hg determination accuracy. Such analysis showed a precision of 4%, as indicated by the relative standard deviation of three replicates, and presented a Hg recovery of $103 \pm 4\%$. The Hg detection limit estimated as three times the standard deviation of reagent blanks, was 1.26 ng g^{-1}. In all cases, blank signals were lower than 0.5% of sample analysis. Concentration values were not corrected for the recoveries found in the certified material.

2.3.3. Evaluating sample quality

There is no general agreement on how to select samples with primary C or O-signals, eliminating those that may have undergone post-depositional change of their isotope values. However, most workers agree that the relative concentration of Mn, Sr, Rb and Fe helps in selecting samples that have undergone little or no alteration (Kaufman and Knoll, 1995; Kha et al., 1999). Among all the parameters used to make such an evaluation, it seems that the most effective is the Mn/Sr ratio, because Sr is preferentially removed during recrystallization of meta-stable carbonate phases, while Mn becomes enriched during formation of late-stage ferroan calcite cement (Ripperdan et al., 1992; Derry et al., 1992; Kaufman et al., 1993; Knoll et al., 1995; Jacobsen and Kaufman, 1999). Although Kaufman and Knoll (1995) stated that limestones or dolostones with Mn/Sr < 10 commonly retain near-primary $\delta^{13}C$ abundances, limestones were here considered to be unaltered only when Mn/Sr < 1.5 and $\delta^{18}O > -10‰$ (PDB) according to Fölling and Frimmel (2002).

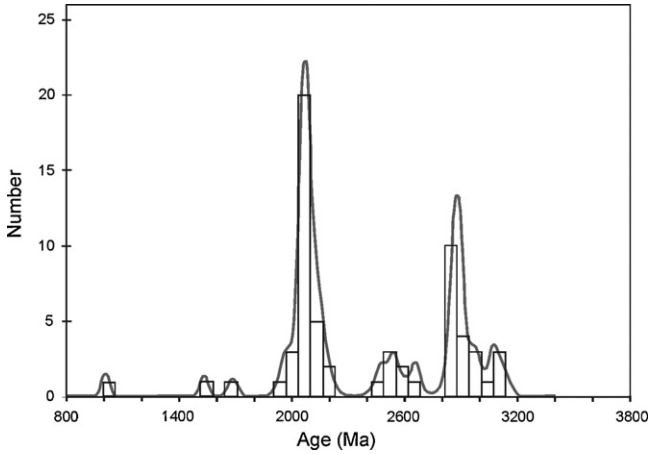

Fig. 11. Histogram of detrital zircon U–Pb LA-MC-ICP-MS age for a sample from the diamictite of the Ribeiropolis Formation at the Capitão Farm, Sergipe.

Table 1
C and O isotopes and some chemical analyses (ppm) of carbonates from the Jacoca Formation, at Capitão Farm, eastern Vaza Barris Domaint, Sergipe.

Sample	Height* (m)	$\delta^{13}C$‰	$\delta^{18}O$‰ PDB	Si × 10^{-3}	Mg/Ca	Mn/Sr	Sr	Rb	Fe × 10^{-3}	$^{87}Sr/^{86}Sr$
JACS-1	0	−6.2	−9.8	1.1	0.25	0.11	111	<10	4.61	
JACS-2	0.30	−4.6	−9.4	2.52	0.27	0.08	140	16	3.19	
JACS-3	0.60	−5.3	−10.1	2.86	0.31	0.09	129	14	2.30	
JACS-4	0.90	−5.0	−11.3	2.82	0.31	0.09	134	16	1.83	
JACS-5	1.20	−4.26	−10.11	3.14	0.27	0.08	147	17	1.74	
JACS-6	1.50	−4.3	−11.3	3.35	0.27	0.11	113	16	1.67	
JACS-7	1.80	−5.3	−12.4	5.05	0.15	0.06	150	18	1.47	
JAC-VB (-1)	3.90	−4.6	−9.0	0.29	0.51	0.61	89	<10	3.81	
JAC-VB-1	8.40	−5.9	−12.9	21.6	0.57	3.33	18	127	5.82	
JAC-VB-2	12.40	−5.9	−10.7	4.64	0.02	3.25	209	10	0.93	
JAC-VB-2	14.40	−4.9	−9.3	4.32	0.04	5.82	170	16	0.57	
JAC-VB-4	17.4	−4.8	−9.1	3.11	0.03	3.0	219	<10	0.41	
JAC-CAP-1	17.6	−4.9	−8.7	5.60	0.02	0.05	3586	12	4411	
JACCAP2/ES	18.2	−4.1	−8.4							
JAC-CAP-3	18.9	−4.1	−8.3							
JAC-CAP-4	19.8	−3.8	−7.5							
JAC-CAP-5	20.3	−4.1	−8.4	5.83	0.08	0.17	1534	23	5.93	
JAC-CAP-6	20.8	−4.9	−8.3							
JAC-CAP-7	20.9	−4.0	−8.6							
JAC-CAP-8	21.5	−4.3	−8.2							
JAC-CAP-9	22.4	−4.5	−8.5							
JAC-CAP-10	23.5	−6.4	−5.6	1.96	0.02	0.03	3044	<10	5.93	
JAC-CAP-11	24.7	−4.2	−8.3	2.35	0.01	0.02	4016	11	2.96	
JAC-CAP-12	27.5	−4.4	−8.2							
JAC-CAP-13	28.3	−4.6	−8.2							
JAC-CAP-14	30.2	−4.0	−8.6							
JAC-CAP-15	31.4	−4.5	−8.7	1.86	0.02	0.09	1676	<10	2.03	
JAC-CAP-16	32.9	−4.1	−8.3							
JAC-CAP-17	37.0	−4.0	−8.1							
JAC-CAP-18	47.6	−3.7	−8.2	3.06	0.01	0.04	1431	<10	1.23	
JAC-CAP-19	67.6	−4.4	−8.5							
JAC-CAP-20	70.1	−3.6	−8.5	3.33	0.02	0.05	3242	<10	1.60	0.707698
JAC-CAP-21	73.1	−3.6	−8.5							
JAC-CAP-22	75.1	−2.9	−7.8	7.72	0.01	0.03	1294	<10	1.99	0.708159
JAC-CAP-23	78.1	−2.9	−7.9							
JAC-CAP-24	79.5	−2.8	−7.7							
JAC-CAP-25	81.5	−2.9	−8.0	11.38	0.02	0.03	2165	<10	1.67	0.708123

* Stratigraphic position in relation to the first sample (JACS-1).

The Mn/Sr ratios for a total of 311 carbonate samples from Jacoca, Olhos D'Agua and Acauã formations in the sections considered here are usually <1.5 when they are limestones. Dolostones usually yielded higher Mn/Sr ratios but most of them are <10. About 95% of the $\delta^{18}O$ values encountered are >−10‰ (PDB). In $\delta^{13}C$ and $\delta^{18}O$ crossplots (not shown) scatter rather than co-variance seems to predominate. These observations imply that the $\delta^{13}C$ values in most of the analyses reported here are primary or near-primary values.

Carbon, oxygen and strontium-isotope analyses and some chemical analyses (ppm) of carbonates from the Acauã, Jacoca and Olhos D'Agua formations are found in Table 1Table 1 through 4, available in a repository with the Precambrian Research editorial office.

2.3.4. Carbon-isotope stratigraphy

In the eastern Vaza Barris Domain, carbonates of the Jacoca Formation at the Capitão Farm (Fig. 6), show negative $\delta^{13}C$ values, mostly between −5 and −4‰ while (^{18}O values are mostly around −8‰ (Table 1, Fig. 12). Shallow-marine dolostone of this formation displays increasing $\delta^{13}C$ values, from −6.2 to −4.3‰, interrupted by a sudden decrease to values of −6.7‰ at the base of the overlying deep shelf limestone succession. Such values shift back to values as high as −1.5‰ in its upper most part. The cap dolostone of this formation shows relatively limited thickness (a couple of meters or less, especially in more distal sections; Fig. 6).

In the western Vaza Barris Domain, detailed C and O isotope chemostratigraphy for the Acauã Formation (São Gonçalo Farm, Borracha and Canabrava Ranges, Patamuté and road Euclides da Cunha-Bendengó) revealed that (^{13}C values tend to group mostly between −5 and −4‰ (Table 2), within the range for mantle values (Hoffman and Schrag, 2002). This highlights the role of mantle-derived CO_2 in carbonate deposition in the aftermath of the glacial event represented by the diamictite of the Juetê Formation.

At Serra da Borracha hill, (^{13}C values remain uniform (around −5‰) for about 165 m (Fig. 13). Only about 1 m of shallow-marine dolostone occurs at the base of the profile (part of the cap dolostones were probably eroded) being followed up section by 30 m of gray, fine-grained limestone with dolostone lonestones (Figs. 6c and 9a and b) and limestone-dolostone rhythmites (Fig. 6d). The (^{18}O values for this interval vary gradually from about −12 to about −5‰. Such enormous fractionation, if primary, likely resulted from a gradual temperature decrease at the level of the dolostone clasts, which may suggest that they are in fact dropstones. Up section, an interval characterized by boudinaged dolostone-limestone intercalations with plane-parallel lamination is observed indicating below wave-base deposition.

Carbonates at Serra da Canabrava Range show (^{13}C values from −6 to −0.2‰ (Table 2) and a package of light gray fine-grained limestone near the Almeida locality nearby Canabrava Range exhibit values from −0.5 to +0.3‰ and seem to be stratigraphically above the carbonate succession at Serra da Borracha.

The nearly identical behavior of C and O isotopes in the Acauã and Jacoca carbonates opens the possibility that they could have been simultaneously deposited, a contention that apparently finds no support in the Sr isotope behavior as discussed later on.

Marly and dolomitic carbonates of the Olhos D'Agua Formation overlying diamictite of the Palestina Formation, near the road Simão Dias-Pinhão (Sergipe), display (^{13}C values as low as −4.7‰, increasing upsection to a plateau between 0 and 1‰ and finally

Table 2
C O and Sr-isotopes and bulk chemical analyses (ppm) of carbonates from the Acauã Formation sampled in six stratigraphic sections at different localities, western Vaza Barris Domain, state of Bahia.

(A) Borracha Range

Sample	Height[a] (m)	$\delta^{13}C‰$ PDB	$\delta^{18}O‰$ PDB	$Si \times 10^{-3}$	Mg/Ca	Mn/Sr	Sr	Rb	$Fe \times 10^{-3}$	$^{87}Sr/^{86}Sr$
SB-06-1	0	−4.84	−13.05	21.79	0.56	15.18	134	<10	2.19	–
SB-06-2	0.6	−4.84	−11.49	7.84	0.01	0.07	2463	<10	0.55	0.70717
SB-06-4	3.6	−4.82	−11.5	6.3	0.01	0.07	2504	<10	0.45	0.70732
SB-06-5	5.1	−5.11	−12.01	38.5	0.03	0.07	2587	<10	3.16	0.70720
SB-06-6	6.1	−4.63	−9.03	4.15	0.01	0.03	2626	<10	0.48	0.70732
SB-06-7	7.1	−4.64	−10.2	15.82	0.01	0.26	1619	<10	0.62	–
SB-06-8	8.6	−3.34	−7.84	5.64	0.59	5.27	222	<10	1.98	–
SB-06-9	11.6	−3.86	−8.96	16.9	0.47	5.25	264	<10	1.77	–
SB-06-10	16.6	−3.28	−6.93	13.58	0.58	7.59	122	<10	1.42	–
SB-06-11	18.6	−4.21	−5.66	28.1	0.59	8.78	125	<10	2.08	–
SB-06-12	20.1	−4.04	−5.41	49.65	0.61	7.59	100	<10	1.74	–
SB-06-13	23.1	−5.36	−8.51	42.6	0.04	3.66	150	<10	0.8	–
SB-06-14	28.1	−4.25	−9.81	70.56	0.04	1.78	294	<10	0.87	–
SB-06-15	33.1	−4	−9.16	14.88	0.08	0.54	322	<10	0.93	–
SB-06-16	37.6	−4.37	−8.06	11.1	0.02	0.32	234	<10	0.62	–
SB-06-17	41.6	−4.02	−8.39	18.9	0.01	0.23	488	<10	1.94	–
SB-06-18	45.6	−4.07	−8.85	7.65	0.04	0.2	646	<10	0.66	–
SB-06-19	49.6	−5.72	−7.55	16.98	0.01	0.81	124	<10	0.97	–
SB-06-20	52.6	−4.02	−8.74	15.58	0.03	0.31	386	<10	1.14	–
SB-06-21	57.6	−5.71	−7.97	14.42	0.02	0.59	119	<10	0.8	–
SB-06-22	61.6	−4.64	−8.05	87.31	0.06	0.66	180	<10	1.18	–
SB-06-23	67.1	−4.3	−7.85	14.14	0.04	0.46	198	<10	1.07	–
SB-06-24	72.1	−4.36	−7.87	14.09	0.03	0.54	142	<10	0.8	–
SB-06-25	78.1	−4.36	−7.7	35.18	0.02	0.31	186	<10	1.42	–
SB-06-27	88.1	−4.73	−8.64	11.85	0.01	0.09	623	<10	0.62	–
SB-06-28	90.6	−5.82	−7.66	23.1	0.04	0.22	273	<10	1.91	–
SB-06-29	90.8	−4.23	−7.09	39.34	0.49	0.56	235	15	3.93	–
SB-06-30	93.3	−5.55	−7.5	30.98	0.07	0.53	119	<10	1.74	–
SB-06-31	96.3	−4.78	−9.55	22.07	0.01	0.95	261	<10	0.8	–
SB-06-32	97.3	−4.79	−7.96	22.35	0.33	6.43	100	<10	2.08	–
SB-06-33	99.3	−5.2	−8.9	111.58	0.09	1.46	223	<10	1.42	–
SB-06-34	103.3	−4.6	−6.52	3.45	0.48	2.22	97	<10	0.87	–
SB-06-35	108.3	−4.8	−6.04	25.43	0.44	7.42	101	<10	1.67	–
SB-06-36	114.3	–	–	–		–		–	–	–
SB-06-37	120.3	−4.78	−9.09	25.1	0.07	1.37	445	<10	1.7	–
SB-06-38	126.3	−4.42	−8.81	17.08	0.06	0.62	353	<10	1.6	–
SB-06-39	130.3	−4.41	−9.4	19.5	0.06	0.54	427	<10	0.62	–
SB-06-40	134.8	−5.01	−8.78	6.67	0.01	1.36	283	<10	0.34	–
SB-06-41	136.8	−4.18	−8.79	10.31	0.29	44.81	57	<10	2.57	–
SB-06-42	146.8	−4.29	−6.71	6.9	0.55	14.13	53	<10	1.46	–
SB-06-43	151.8	−6.71	−5.87	2.75	0.25	27.14	21	<10	1.04	–
SB-06-44	165.8	−5.04	−6.68	2.98	0.35	10.94	51	<10	0.73	–

(B) São Gonçalo Farm, near Euclides da Cunha village

Sample	Height[b] (m)	$\delta^{13}C‰$ PDB	$\delta^{18}O‰$ PDB	$Si \times 10^{-3}$	Mg/Ca	Mn/Sr	Sr	Rb	$Fe \times 10^{-3}$	Hg ($ng\,g^{-1}$)	$^{87}Sr/^{86}Sr$
EC-SG 01	0	−4.9	−4.64	11.48	0.47	49.7	27	<10	5.63	22.9	
EC-SG 02	0.5	−3.3	−6.22	2.57	0.47	20.3	52	10	4.75	11	
EC-SG 03	1	−3.7	−5.16	5.6	0.57	62.0	25	<10	6.99	10.9	
EC-SG 04	2	−3.6	−5.71	5.37	0.57	26.8	38	<10	5.26		
EC-SG 05	3	−3.7	−6.26	8.68	0.47	35.2	31	<10	5.39	23.1	0.70994
EC-SG 06	4	−3.5	−6.78	20.58	0.51	27.4	40	11	6.39		
EC-SG 07	5	−3.5	−6.78	21.56	0.51	17.1	59	12	6.84	15	0.71099
EC-SG 08	6	−3.4	−5.96	33.04	0.59	24.2	40	18	7.34		
EC-SG 09	7	−4.1	−6.41	26.74	0.53	17.7	46	16	6.85	15.1	
EC-SG 10	8	−3.2	−5.92	46.39	0.61	22.1	41	18	21.84		
EC-SG 11	9	−3.4	−5.39	66.41	0.63	20.2	47	27	10.86	23.1	
EC-SG 12	10	−3.1	−5.45	76.91	0.65	22.4	27	34	48.25		
EC-SG 13	11	−2.9	−6.42	55.91	0.62	15.3	49	25	11.23	19.8	0.71012
EC-SG 14	12	−2.9	−6.35	44.61	0.60	14.7	54	21	12.99		
EC-SG 15	13	−2.9	−6.29	45.45	0.60	15.1	61	22	11.21	26.2	0.70942
EC-SG 16	14	−2.93	−5.95	52.55	0.61	14.9	56	28	12.11	22.4	0.71063

(C) Patamuté village

Sample	Height[c] (m)	$\delta^{13}C‰$ PDB	$\delta^{18}O‰$ PDB	$Si \times 10^{-3}$	Mg/Ca	Mn/Sr	Sr	Rb	$Fe \times 10^{-3}$	Hg ($ng\,g^{-1}$)	$^{87}Sr/^{86}Sr$
PATAA	0	−3.8	−9.89	1.48	0.08	5.78	292	<10	–	10.9	0.70751
PATA B	0.3	−5.04	−5.84	1.47	0.40	11.26	137	15	–	15.1	
PATA C	2.3	−4.88	−6.47	1.63	0.52	8.85	165	<10	–	14.9	0.70809
PATA 1	3.8	−3.66	−10.67	8.02	0.07	6.66	282	<10	2.98	11.2	0.71001
PATA 2	4.8	−3.78	−10.41	4.27	0.08	7.45	219	<10	3.12	10.9	
PATA 3	5.8	−4.02	−5.07	4.35	0.51	27.55	78	10	8.69	10.9	0.70883

Table 2 (*Continued*)

(C) Patamuté village

Sample	Height[c] (m)	$\delta^{13}C$‰ PDB	$\delta^{18}O$‰ PDB	Si × 10^{-3}	Mg/Ca	Mn/Sr	Sr	Rb	Fe × 10^{-3}	Hg (ng g^{-1})	$^{87}Sr/^{86}Sr$
PATA 4	6.8	−6.07	−10.2	3.52	0.14	3.59	258	23	12.52	23.1	
PATA 5	7	−6.5	−10.35	6.64	0.26	2.75	317	10	4.45	41.8	
PATA 6	8	−6.6	−10.4	8.10	0.39	3.72	316	11	6.29		
PATA 7	8.5	−6.87	−10.59	5.65	0.07	6.69	268	<10	9.36	10.8	
PATA 8	9	−7.2	−10.82	6.61	0.29	4.09	361	12	7.09		
PATA 9	9.5	−7.27	−10.88	7.42	0.24	4.65	429	11	6.83	15	
PATA 10	10	−6.86	−10.65	8.76	0.53	4.47	371	<10	7.62		
PATA 11	10.5	−7.34	−10.41	6.62	0.21	4.53	451	13	6.97	11	
PATA 12	11	−7.99	−10.62	7.42	0.29	10.59	339	19	12.37		0.71115
PATA 13	12	−8.09	−7.87	8.76	0.18	16.41	246	12	7.18		
PATA 14	13.5	−9.06	−7.38	4.73	0.29	5.30	295	15	9.59		0.70937
PATA 15	14.5	−7.14	−10.76	7.79	0.40	2.22	550	10	6.39	15	
PATA 16	16.5	−5.28	−9.99	5.89	0.09	2.40	557	10	7.99	15	0.70880

(D) Road Euclides da Cunha village to Bendegó village

Sample	Height[d] (m)	$\delta^{13}C$‰ PDB	$\delta^{18}O$‰ PDB	Si × 10^{-3}	Mg/Ca	Mn/Sr	Sr	Rb	$^{87}Sr/^{86}Sr$
ECBR 1	0	−6.92	−11.53	5.81	0.22	2.84	416	10	0.70852
ECBR 2	6.5	−8.08	−8.72	4.75	0.16	4.05	261	10	
ECBR 3	11.2	−6.53	−10.55	4.26	0. 16	4.28	392	10	0.70854
ECBR 4	17.5	−7.01	−11.2						0.70791
ECBR 5	22.3	−7.27	−6.95	3.37	0.08	6.13	267	<10	
ECBR 6	25.8	−6.72	−9.75	6.33	0.15	5.96	329	<10	
ECBR 7	55.8	−6.03	−9.43	2.78	0.14	0.96	971	<10	0.70522
ECBR 8	58.8	−5.72	−9.57	3.90	0.26	1.56	719	<10	
ECBR 9	60.8	−6.35	−9.68	2.95	0.12	2.88	384	<10	0.70795
ECBR 10	63.3	−6.24	−7.7	3.99	0.11	2.76	412	<10	0.70763
ECBR 11	66.3	−5.92	−9.4	4.13	0.14	2.15	695	<10	
ECBR 12	68.3	−5.77	−9.61	16.27	0.33	1.16	832	<10	0.70762
ECBR 13	70.8	−5.64	−9.42	2.66	0.15	4.04	375	<10	
ECBR 14	73.3	−5.79	−9.12	2.74	0.09	3.07	418	<10	
ECBR 15	75.3	−5.59	−9.31	2.56	0.14	1.73	663	<10	0.70778

(E) Araçá Quarry, near Euclides da Cunha village

Sample	Height[e] (m)	$\delta^{13}C$‰ PDB	$\delta^{18}O$‰ PDB	Si × 10^{-3}	Mg/Ca	Mn/Sr	Sr	Rb	Fe × 10^{3}
ECPA 1	0	−1.2	−6.26	7.20	0.23	0.27	590	26	8.74
ECPA 2	1	−1.64	−8.32	13.71	0.05	0.09	748	<10	4.53
ECPA 3	2	−0.94	−8.37	1.33	0.09	0.02	2084	<10	1.71
ECPA 4	3	−0.93	−8.48	1.56	0.15	0.03	1332	<10	1.72
ECPA 5	4	−0.91	−5.3	9.76	0.05	0.43	462	17	11.00
ECPA 6	5	−1.25	−7.95	4.85	0. 12	0.20	627	<10	5.31
ECPA 7	6	−0.99	−8.4	1.42	0.14	0.03	1333	<10	1.32
ECPA 8	7	−0.58	−8.07	1.78	0.11	0.01	2370	<10	1.33
ECPA 9	8	−1.01	−7.42	0.59	0.69	0.01	3719	<10	1.21
ECPA 10	9	−1.72	−7.62	0.49	0.84	0.02	2752	<10	1.37
ECPA 11	10	−1.41	−7.14	7.05	0. 15	0.15	955	20	8.13
ECPA 12	11	−1.19	−6.66	8.59	0. 28	0.35	574	28	11.51
ECPA 13	12	−0.84	−7.62	0.88	0.74	0.01	3511	<10	1.27
ECPA 14	13	−0.89	−8.06	0.61	0.53	0.01	3889	<10	1.10
ECPA 15	14	−0.86	−7.72	0.58	0.48	0.01	3754	<10	1.07
ECPA 16	15	−1.05	−8.04	0.95	0.77	0.01	2259	<10	1.08
ECPA 17	16	−1.38	−8.14	2.49	0.99	0.07	877	<10	2.10
ECPA 18	18	−1.38	−8.18	2.38	0.13	0.03	1311	<10	1.61

(F) Bendegó village

Sample	Height[f] (m)	$\delta^{13}C$‰ PDB	$\delta^{18}O$‰ PDB	Si × 10^{-3}	Mg/Ca	Mn/Sr	Sr	Rb	Fe × 10^{-3}
BCV 01	0	−2.01	−10.91	8.79	0.16	0.67	829	10	7.75
BCV 02	1	−0.77	−8.41	5.72	0.36	1.02	664	17	7.66
BCV 03	2	0.05	−10.21	4.71	0.11	0.40	899	13	5.03
BCV 04	3	0.62	−9.29	8.00	0.08	0.58	795	11	8.31
BCV 05	4	2.39	−10.94	6.85	0.06	0.18	1337	<10	4.70
BCV 06	6	2.16	−12.74	9.79	0.05	0.13	1775	11	5.92
BCV 07	7	0.01	−10.78	7.43	0.10	0.13	1265	14	4.43
BCV 08	8	−0.19	−10.58	7.72	0.12	0.36	1292	<10	3.82
BCV 09	9	−0.37	−10.08	8.23	0.23	0.26	704	<10	5.03
BCV 10	10	−1.89	−10.1	6.59	0.17	0.40	797	<10	5.89
BCV 11	11	−2.06	−9.84	8.98	0.16	0.42	750	<10	7.15
BCV 12	12	−0.31	−9.85	10.14	0.30	0.35	751	14	6.13
BCV 13	13	−0.01	−10.21	6.31	0.08	0.18	1203	<10	5.47
BCV 14	14	0.1	−9.85	12.84	0.16	0.60	791	28	9.88
BCV 15	15	−0.02	−9.09	9.38	0.23	0.45	677	17	7.69
BCV 16	16	−0.89	−9.34	12.49	0.10	0.56	571	26	9.62

Table 2 (*Continued*)

(F) Bendegó village

Sample	Height[f] (m)	$\delta^{13}C$‰ PDB	$\delta^{18}O$‰ PDB	Si × 10^{-3}	Mg/Ca	Mn/Sr	Sr	Rb	Fe × 10^{-3}
BCV 17	17	−0.74	−9.73	7.59	0.10	0.35	870	<10	3.53
BCV 18	18	−0.27	−10.09	5.64	0.10	0.25	977	21	4.73
BCV 19	19	−0.36	−10.48	9.57	0.12	0.20	1002	15	4.32
BCV 20	20	−0.75	−10.43	10.54	0.09	0.51	790	18	7.53
BCV 21	21	−1.95	−10.28	7.87	0.10	0.35	797	<10	4.50
BCV 22	22	−2.12	−10.22	13.88	0.01	0.59	634	19	9.00
BCV 23	23	−1.75	−10.08	8.71	0.08	0.36	841	15	7.47
BCV 24	25	−1.99	−9.59	11.36	0.20	0.93	614	18	9.49
BCV 25	27	−2.03	−10.09	7.14	0.12	0.84	696	<10	4.92

(G) Canabrava Range

Sample	Height[g] (m)	$\delta^{13}C$‰ PDB	$\delta^{18}O$‰ PDB	Si × 10^{-3}	Mg/Ca	Mn/Sr	Sr	Rb	Fe × 10^{-3}
CANAB-1	0	−2.14	−13.09	–	–	–	–	–	–
CANAB-2	100	−0.24	−8.14	1.86	0.12	0.12	746	<10	0.03
CANAB-3	110	−1.81	−8.88	4.63	0.07	0.04	590	<10	0.04
CANAB-4	134	−1.87	−7.88	2.84	0.12	0.05	646	<10	0.04
CANAB-4A	165	−0.27	−8.29	0.70	0.01	0.01	4680	<10	0.04
CANAB-5	167	−0.21	−8.26	0.80	0.01	0.01	4426	<10	0.05
CANAB-6	180	−0.24	−8.14	0.56	0.01	0.01	4765	<10	0.07
CANAB-7	210	−0.87	−8.03	4.61	0.01	0.01	3424	<10	0.08
CANAB-8	235	−1.39	−7.92	0.65	0.06	0.01	1462	<10	0.03
CANAB-9	240	−1.63	−6.38	0.76	0.20	0.08	672	<10	0.04
CANAB-10	309	−1.46	−8.3	4.81	0.02	0.01	1795	<10	0.03
CANAB-11	311	−1.46	−7.39	0.29	0.11	0.04	1019	<10	0.03
CANAB-12A (white)	313	−6.11	−7.95	0.92	0.01	0.23	366	<10	0.02
CANAB-12B (dark)	314.5	−4.51	−7.19	0.97	0.01	0.05	643	<10	0.02
CANAB-13	315.5	–	–	1.06	0.40	0.11	447	<10	0.06
CANAB-14	318.5	−1.84	−6.75	1.56	0.03	0.17	326	<10	0.04
CANAB-15	320.5	−1.3	−7.75	6.15	0.05	0.01	963	<10	0.02
CANAB-16	322.5	−0.87	−7.61	17.08	0.16	0.04	1029	<10	0.10
CANAB-17	325.5	−1.02	−7.7	0.02	0.08	0.03	699	<10	0.03
CANAB-18	327	−0.69	−8.04	1.33	0.06	0.02	988	<10	0.03
CANAB-19	330	−0.64	−9.99	1.40	0.03	0.01	2111	<10	0.03
CANAB-20	332	−1.62	−7.44	5.52	0.05	0.03	934	<10	0.03

(H) Almeida Farm, nearby Canabrava Range

Sample	Height[h] (m)	$\delta^{13}C$‰	$\delta^{18}O$‰ PDB
ALM-1	0	−0.18	−6.19
ALM-2	12.5	−0.54	−5.98
ALM-3	28.5	−0.42	−9.90
ALM-4	42.5	−2.01	−7.28
ALM-5	61.5	−0.54	−8.36
ALM-6	73.8	−0.78	−8.36
ALM-7	81.6	−1.18	−7.91
ALM-8	109.6	−0.75	−8.28
ALM-9	123.6	+0.27	−8.56
ALM-10	138.1	−0.09	−8.60

[a] Stratigraphic position in relation to the first sample (SB-06-1) of the section.
[b] Stratigraphic position in relation to the first sample (EC-SG-01) of the section.
[c] Stratigraphic position in relation to the first sample (PATA A) of the section.
[d] Stratigraphic position in relation to the first sample (ECBR1) of the section.
[e] Stratigraphic position in relation to the first sample (ECPA1) of the section.
[f] Stratigraphic position in relation to the first sample (BCV01) of the section.
[g] Stratigraphic position in relation to the first sample (CANAB-1) of the section.
[h] Stratigraphic position in relation to the first sample (ALM-1) of the section.

to another plateau around +8 to +10‰ (Table 3). This pattern is observed in the sections at the Capitão Range, at the section in the Rosario-Cocorobó road (Bahia) and between Simão Dias and Pinhão villages (Sergipe) (Table 3, Figs. 14 and 15). The (^{18}O values in these sections vary from −7 to −11‰ and (^{13}C from −5 to +9‰. Low Mn/Sr and lack of co-variance between (^{13}C values and Mn/Sr values suggest that these isotopic values are primary.

A section of the Olhos D'Agua Formation near Rosário village, Bahia, shows an intercalation of limestone and siltstone, where the carbonate lenses show variable thickness. These carbonates have been deposited on top of diamictite of the Palestina Formation, the latter comprising pebbles, boulders and blocks of granite, gneiss, black phyllite, black chert, greenish quartzite and gray limestone. The (^{13}C values start with slightly negative values (∼−2‰) and about 10 m from the base, values change dramatically and form a well-defined plateau around +9‰, while the (^{18}O values vary from −10 to −12‰.

2.3.5. *Strontium-isotope stratigraphy*

Sr isotope ratios have been analyzed in 40 carbonate samples from the Sergipano Belt including samples from the Acauã Formation (Borracha, Patamuté, São Gonçalo, Euclides da Cunha) and Olhos D'Agua Formation (Rosario and Capitão Hill) in the western Vaza Barris Domain and Jacoca Formation (Capitão Farm) and Olhos D'Agua Formation (road Simão Dias-Pinhão) in the eastern Vaza Barris Domain. Typically, carbonate samples with high Sr

Table 3
C and O isotopes and chemistry (ppm) of carbonates from Olhos D'Agua Formation, road Simão Dias–Pinhão, eastern Vaza Barris Domain, in Sergipe.

Sample	Height*(m)	$\delta^{13}C‰$	$\delta\ ^{18}O‰_{PDB}$	$Si \times 10^{-3}$	Mg/Ca	Mn/Sr	Sr	Rb	$Fe \times 10^{-3}$	$^{87}Sr/^{86}Sr$
2-OD – 01	24.7	−2.4	−9.9	92.63	0.18	0.63	443	14	7.67	
2-OD – 02	26.4	−2.6	−10.1							
2-OD – 03	28.0	−2.3	−9.7							
2-OD – 04	29.4	−3.6	−8.0							
2-OD – 05	32.5	2.0	−9.3							
2-OD – 06	34.2	−2.2	−9.5							
2-OD – 07	35.4	−7.0	−9.8							
2-OD – 08	37.9	−4.9	−5.9							
2-OD – 09	41.4	−1.9	−9.2							
2-OD – 10	42.3	−1.9	−9.3	44.40	0.07	0.18	784	<10	3.45	
2-OD – 11	43.5	−2.0	−9.3							
2-OD – 12	45.7	−1.9	−8.5							
2-OD – 13	46.7	−1.7	8.6							
2-OD – 14	48.3	−1.0	−8.4							
2-OD – 15	50.1	−3.3	−7.8							
2-OD – 16	51.4									
2-OD – 17	53.3	−2.0	−9.4							
2-OD – 18	54.9	−7.5	−4.6							
2-OD – 19	59.1	−1.3	−8.6							
2-OD – 20	60.0	−1.2	−8.5							
2-OD – 21	61.2	−0.4	−7.4	9.93	0.01	0.01	2281	<10	0.91	
2-OD – 22	61.6	−0.1	−7.6							
2-OD – 23	62.1	−0.2	−8.3							
2-OD – 24	63.9	−0.8	−8.9	26.61	0.06	0.04	1297	<10	2.01	
3-OD – 01	64.9	−1.1	−7.4	54.15	0.13	0.09	899	<10	2.83	0.707986
3-OD-02 dark	65.7	−2.4	−7.6							
3-OD-02 white	66.5	−0.4	−7.9							
3-OD – 03	68.1	−1.1	−7.7							
3-OD – 04	69.7	−3.5	−6.1	71.62	0.03	0.12	854	10	3.42	0.707999
3-OD – 05	72.7	−4.7	−9.9							
3-OD – 06	77.1	−0.4	−7.8	19.28	0.01	0.01	2564	<10	0.90	0.707781
3-OD – 07	81.4	−0.1	−8.3							
3-OD – 08 A	84.6	−4.2	−7.1							
3-OD – 08 B	87.8	−3.2	−7.2							
3-OD – 08 c	91.0	−0.7	−7.5	81.74	0.14	0.29	895	23	6.25	
3-OD – 09	92.7	−4.1	−6.0							
3-OD – 10	93.3	−0.8	−6.5							
3-OD – 11	94.6	−0.5	6.7							
3-OD – 12	95.3	−0.6	−6.4							
3-OD – 13	99.3	−0.4	−6.3	66.62	0.39	0.40	552	23	4.46	
3-OD – 14	103.4	−0.2	−0.7							
3-OD – 15	104.6	0.1	−6.9							
3-OD – 16	108.0	−0.2	−7.7							
3-OD – 17	114.1	−0.2	−7.1	94.96	0.35	0.86	451	16	6.89	
5-OD – 01	115.1	−0.3	−8.2	82.37	0.07	0.021	1032	24	4.21	
5-OD – 02	119.1	−0.5	−7.5							
5-OD - 03	124.3	−0.5	−6.3							
5-OD – 04	127.4	−0.5	−7.2							
5-OD – 05	130.2	−0.7	−8.3	26.86	0.08	00.05	1359	<10	1.49	
5-OD – 06	132.9	0.8	−8.4							
5-OD – 07	136.9	−0.3	−8.3							
5-OD – 08	140.4	−1.7	−8.4							
5-OD – 09	143.9	0.3	−8.0							
5-OD – 10	153.7	−1.0	−8.1	36.76	0.05	0.05	1356	<10	1.56	
5-OD – 11	157.5	−0.6	−9.7							
5-OD – 12	160.6	−1.7	−8.1							
5-OD – 13	165.2	−0.4	−8.7							
5-OD – 14	167.6	−0.6	−8.6							
5-OD – 15	170.0	−0.6	−8.1	29.06	0.09	0.05	1349	<10	1.41	
5-OD – 16	176.0	−2.2	−9.7							
5-OD – 17	182.3	−0.1	−8.7							
5-OD – 18	188.3	−0.1	−9.0							
5-OD – 19	194.7	0.8	−9.0							
5-OD – 20	196.3	−0.7	−9.2	45.48	0.15	0.08	1436	<10	2.44	
5-OD – 21	201.3	−0.2	−9.2							
5-OD – 22	206.8	−0.1	−8.9							
5-OD – 23	216.4	−1.2	−8.4							
5-OD – 24	218.1	−0.5	−9.5							
5-OD – 25	224.9	−0.7	−7.4							
5-OD – 26	231.4	−0.8	−9.0	2.99	0.01	0.018	3980	<10	0.57	
5-OD – 27	238.5	2.0	−9.4							
5-OD – 28	247.5	−1.9	−10.2							
5-OD – 29	252.5	−2.4	−9.5							
5-OD – 30	254.8	−2.3	−9.7	46.63	0.04	0.10	1528	<10	2.13	
5-OD – 31	263.8	−1.5	−8.2							

Table 3 (*Continued.*)

5-OD – 32	272.1	−1.6	8.3						
5-OD – 33	280.4	0.8	−8.2						
5-OD – 34	291.1	−0.2	−8.0						
5-OD – 35	303.9	−0.2	−7.8	57.27	0.06	0.18	1061	22	3.22
5-OD – 36	314.9	0.3	−7.7	41.07	0.13	0.15	948	13	2.52
5-OD – 37	324.5	1.6	−8.2						
5-OD – 38	330.6	9.0	−7.2	5.19	0.01	0.15	1172	<10	2.51
5-OD – 39	336.9	8.7	−8.0						
5-OD – 40	348.2	9.0	−7.8	4.67	0.01	0.05	1449	<10	0.97
5-OD – 41	357.2	2.3	−6.6	17.83	0.01	0.06	1285	11	3.25
5-OD – 42	365.1	5.6	−7.7						
5-OD – 43	369.9	6.3	−7.7	8.18	0.01	0.17	2421	<10	1.76
5-OD – 44	377.6	8.6	−8.3						
5-OD – 45	387.3	9.9	−8.3						
5-OD – 46	394.3	10.1	−6.7	3.49	0.01	0.02	2463	<10	1.44
5-OD – 47	398.9	10.0	7.7						
5-OD – 48	408.0	11.0	−6.5	10.37	0.01	0.02	2876	<10	1.38
5-OD – 49	414.6	8.2	−7.0						
5-OD – 50	424.2	10.9	−6.7	4.12	0.01	0.07	2755	<10	1.06
5-OD – 51	427.2	9.2	−7.3						
5-OD – 52	430.8	10.9	−6.1						
5-OD – 53	441.5	8.7	−9.2						
5-OD – 54	451.1	8.9	−7.6						
5-OD – 55	461.5	10.3	−7.6	3.91	0.01	0.15	2615	<10	1.51
5-OD – 56	468.2	10.3	−7.9						
5-OD – 57	475.8	10.3	−9.1						
5-OD – 58	488.1	10.2	−8.3						
5-OD – 59	492.8	9.1	−8.0						
5-OD – 60	503.8	9.8	−7.5						
5-OD – 61	519.0	8.5	−7.5	7.73	0.01	0.02	2615	<10	1.47

* Stratigraphic position in relation to the first sample (2-OD-01).

(>600 ppm), low Rb (<10 ppm), low Mn/Sr (<10) and low Mg/Ca (<0.2) ratios have been considered for Sr isotope ratio analysis since usually samples which meet these requirements yield consistent $^{87}Sr/^{86}Sr$ Sr ratios. However, when dolomite was the only carbonate present (Mg/Ca around 0.6), consistency of the $^{87}Sr/^{86}Sr$ ratios was the only selection criterion.

Strontium-isotope ratios for the Jacoca Formation at the Capitão Farm are reported in Table 1; for the Acauã Formation in sections at Serra da Borracha, São Gonçalo, Patamuté village and in the Road Euclides da Cunha-Bedengó, in Table 2, and for the Olhos D'Agua Formation in a section near Pinhão village in Table 3 and, Capitão Hill and Rosario, in Table 4.

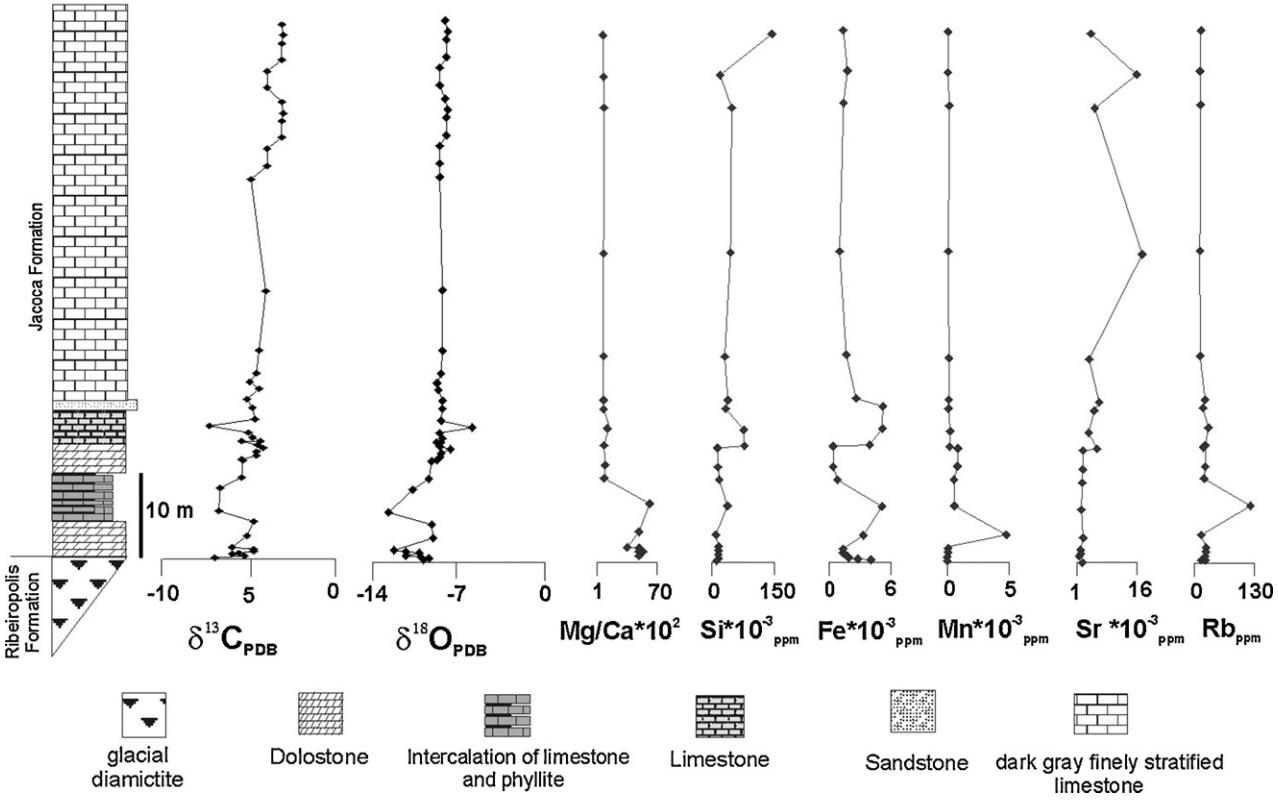

Fig. 12. C and O-isotope and chemical stratigraphies for Jacoca Formation carbonates at the Capitão Farm, by the Vaza Barris River, Sergipe.

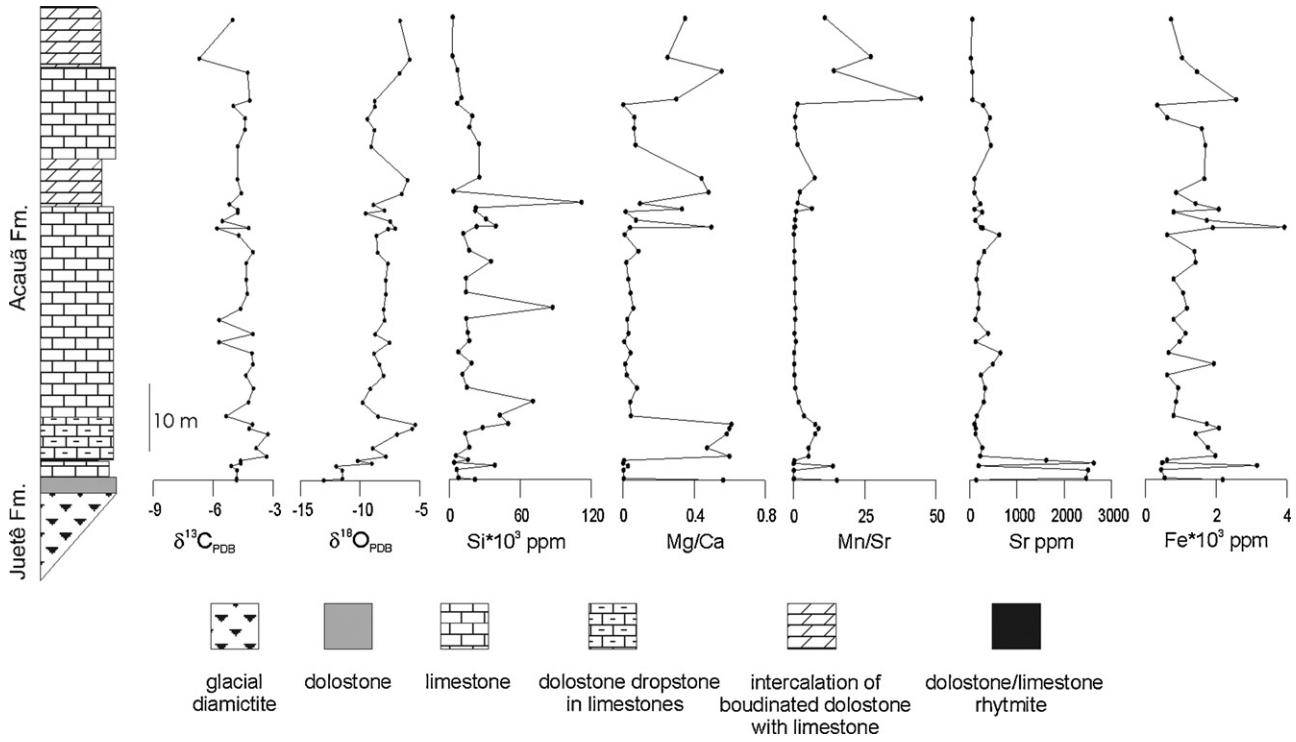

Fig. 13. Litho- and chemostratigraphy for the Acauã Formation at the Serra da Borracha range, at about 20 km west from Patamuté village, Bahia.

Carbonates of the Jacoca Formation display values of $^{87}Sr/^{86}Sr$ of 0.7077, 0.7081 and 0.7081 at Capitão Farm. Four analyses of carbonates of the Acauã Formation yielded consistent results at the Serra da Borracha (two values of 0.7072 and two of 0.7073) but very variable and higher values at the three other localities examined in the western Vaza Barris Domain (all dolostones). Three $^{87}Sr/^{86}Sr$ ratios for high Sr carbonates of the Olhos D'Agua Formation in the section near Pinhão village yielded values of 0.7078, 0.7080 and 0.7080.

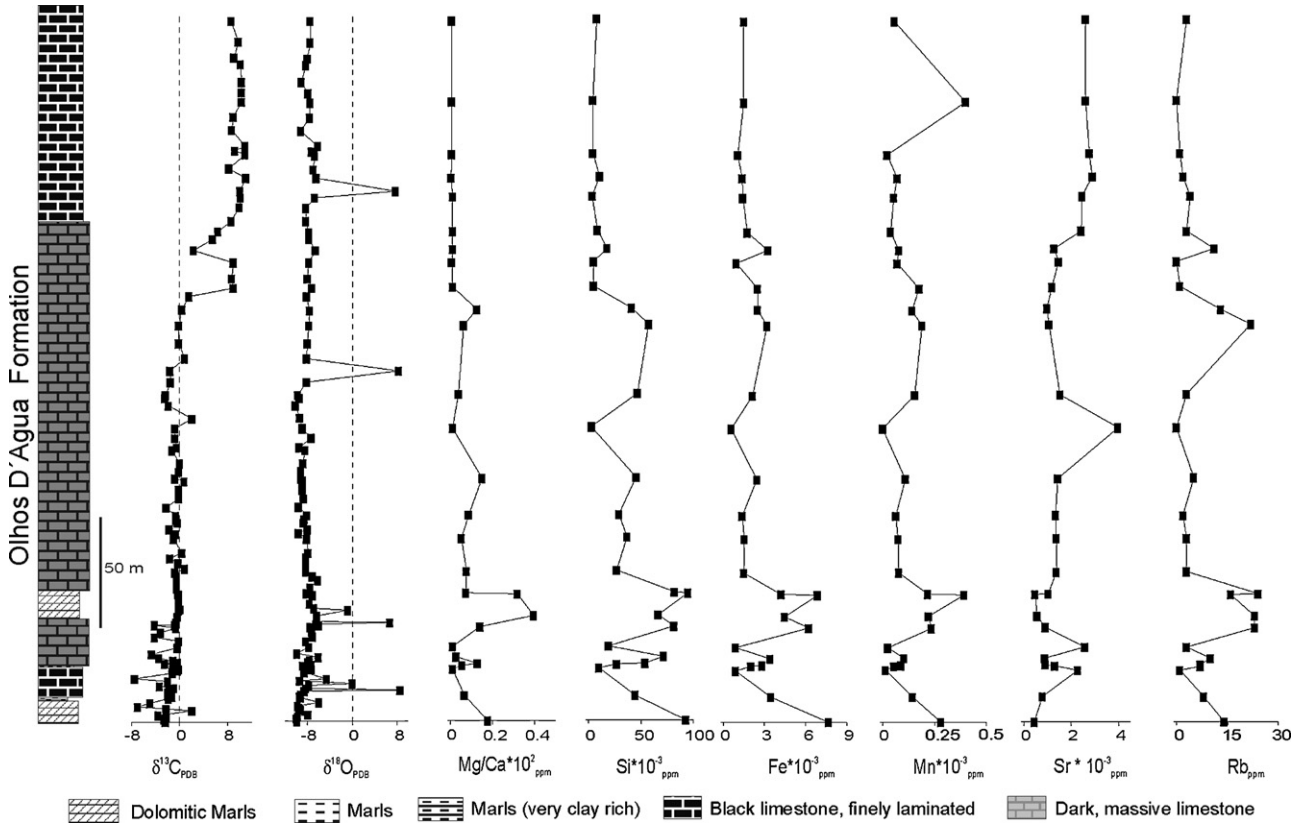

Fig. 14. Composite chemostratigraphic profile for the Olhos D'Agua Formation using three sections by the road Simão Dias-Pinhão, Sergipe.

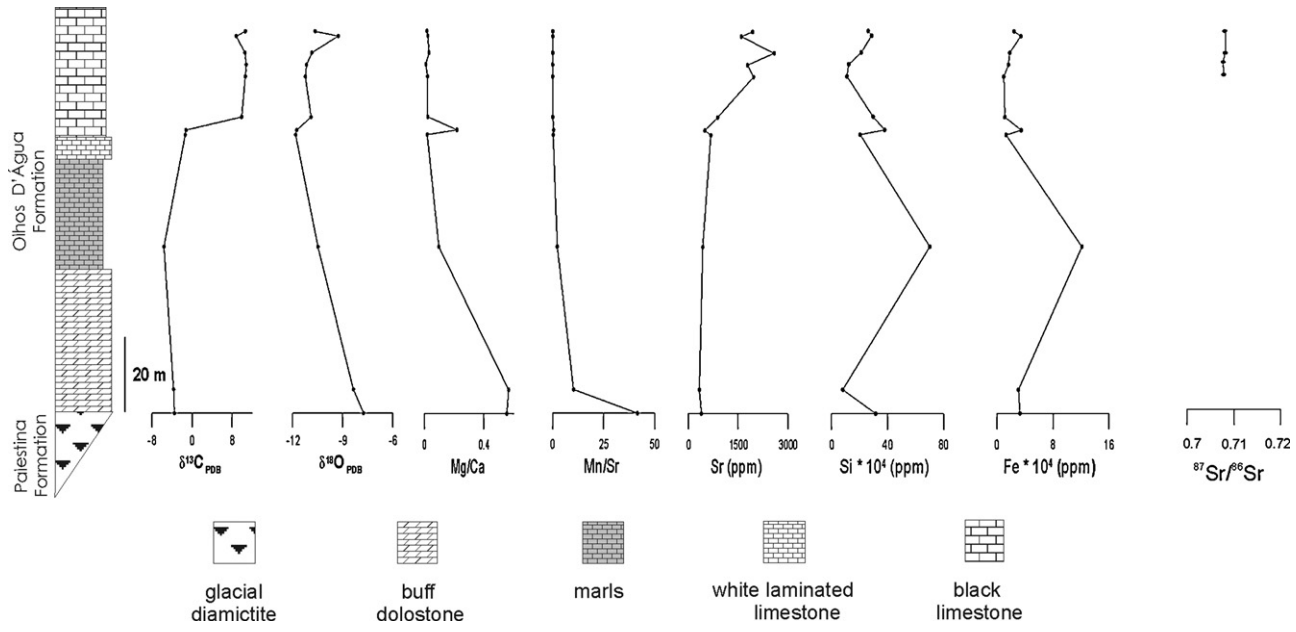

Fig. 15. Litho- and chemostratigraphy for the Olhos D'Agua Formation at the Capitão Range, Bahia.

At Capitão Range, carbonates of this formation displayed values of 0.7077–0.7081 and from 0.7077–0.7082 at the section near Rosario Village. All these $^{87}Sr/^{86}Sr$ ratios are within the range of late Neoproterozoic seawater (0.7060–0.7090), as pointed out by Kaufman et al. (1993, 2009).

Therefore, carbonates of the Olhos D'Agua Formation from three localities examined (eastern and western Vaza Barris domains) show nearly the same range of $^{87}Sr/^{86}Sr$ ratios, indistinguishable from that of the Jacoca Formation at the Capitão Farm. However, $^{87}Sr/^{86}Sr$ ratios for the Serra da Borracha range are consistently

Table 4
C, O and Sr-isotopes and chemistry (ppm) of carbonates from the Olhos D'Agua Formation, at the western Vaza Barris Domain, state of Bahia.

(A) Capitão Range, near Paripiranga

Sample	Height[a] (m)	$\delta^{13}C$‰PDB	$\delta^{18}O$‰ PDB	Si × 10^4	Mg/Ca	Mn/Sr	Sr	Rb	Fe × 10^4	$^{87}Sr/^{86}Sr$
SCAP-1A	0	−3.51	−7.75	31.50	0.55	41.63	398	11	3.27	–
SCAP-1B	10	−3.67	−8.36	7.91	0.56	10.30	335	<10	3.07	–
SCAP-2	70	−5.59	−10.48	70.14	0.10	2.35	437	39	12.15	–
SCAP-3	117	−1.35	−11.81	20.42	0.02	0.31	679	<10	1.29	–
SCAP-4	119	−1.2	−11.74	37.93	0.22	0.55	503	10	3.48	–
SCAP-5	124.5	9.92	−10.89	29.61	0.02	0.14	884	<10	1.12	–
SCAP-6	141.5	10.64	−11.23	10.91	0.02	0.10	1967	<10	0.98	0.70787
SCAP-7	146.5	10.83	−11.16	12.19	0.01	0.08	1785	<10	1.64	0.70773
SCAP-8	151.5	10.57	−10.84	21.15	0.03	0.13	2588	<10	1.81	0.70815
SCAP-9	158.5	8.81	−9.27	28.52	0.02	0.14	1597	11	3.39	–
SCAP-10	160.5	10.65	−10.65	26.10	0.02	0.11	1938	<10	2.44	0.70816

(B) Rosario village

Sample	Height[b] (m)	$\delta^{13}C$‰ PDB	δ^{18}(‰ PDB	Si × 10^{-3}	Mg/Ca	Mn/Sr	Sr	Rb	Fe × 10^{-3}	$^{87}Sr/^{86}Sr$
ROSA 1	13.2	−0.09	−11.31	11.24	0.11	6.61	936	5	0.28	0.70914
ROSA 2	33.2	0.59	−7.63	5.69	0.46	10.84	511	17	0.46	
ROSA 3	40.9	−0.41	−8.27	7.88	0.19	9.60	698	9	0.47	
ROSA 4	51.4	5.07	−11.39	6.74	0.03	6.02	2018	11	0.63	0.70828
ROSA 5	112.9	7.17	−10.58	4.29	0.02	1.75	1793	21	0.63	
ROSA 6	121	7.2	−11.43	4.13	0.02	1.34	2172	16	0.49	0.70773
ROSA 7	130.5	6.9	−12.75	3.58	0.0	2.85	2048	8	0.50	
ROSA 8	141.8	8.12	−12.04	2.19	0.02	1.55	2037	15	0.70	0.70897
ROSA 9	146.1	8.12	−12.26	6.90	0.02	1.42	2388	14	0.64	
ROSA 10	328.1	9.5	−11.01	0.80	0.51	0.60	2185	<10	0.09	0.70753
ROSA 11	358.1	9.04	−11.41	0.59	0.54	0.71	1972	<10	0.07	
ROSA 12	389.1	9.55	−11.49	0.80	0.26	0.44	2313	<10	0.12	0.70761
ROSA 13	413	9.33	−11.39	0.60	0.48	0.58	2199	<10	0.05	
ROSA 14	491.4	9.34	−2.97	5.34	0.08	4.14	2211	<10	0.07	
ROSA 15	503.4	8.63	−11.63	1.29	0.50	0.64	2096	<10	0.12	
ROSA 16	550.8	9.45	−11.72	0.82	0.49	0.92	2397	<10	0.15	
ROSA 17	599.5	9.22	−10.82	0.98	0.51	1.06	2180	<10	0.07	
ROSA 18	630.5	9.46	−11.55	3.40	0.07	1.51	2646	<10	0.08	

[a] Stratigraphic position in relation to the first sample (SCAP-1A) of the section.
[b] Stratigraphic position in relation to the first sample (ROSA 01) of the section.

lower than those for the Jacoca Formation, in contrast with $\delta^{13}C$ values that tend to fall in the same range for these two formations (virtually all negative).

Kaufman et al. (2009) has compiled $^{87}Sr/^{86}Sr$ ratios for limestones in cap lithofacies across southwestern Gondwana and they seem to fall consistently within three modes with values near 0.7066, 0.7073 and 0.7081 represented respectively by the Rasthof, Maieberg and Bildah cap carbonates in Namibia and their temporal equivalents. In this scheme of Kaufman et al. (2009), $^{87}Sr/^{86}Sr$ ratios for the Acauã Formation carbonates at the Serra da Borracha (0.7073) approach $^{87}Sr/^{86}Sr$ ratios for Sturtian II cap carbonates deposited between 740 and 635 Ma. In addition, similarly to the Maieberg cap carbonate, $\delta^{13}C$ values at the Serra da Borracha are virtually all negative.

However, $^{87}Sr/^{86}Sr$ ratios as low as 0.7073 have been reported from Ediacaran, *Cloudina*-bearing limestones in Uruguay (Gaucher et al., 2004, 2009) and are also similar to $^{87}Sr/^{86}Sr$ values of post-Marinoan carbonates in NW Canada, NW Namibia and SW Brazil (Halverson et al., 2007).

The range of $^{87}Sr/^{86}Sr$ ratios for the Jacoca and Olhos D'Agua formations are similar to each other (0.7077–0.7081), in consonance with values reported for the terminal Cryogenian Bildah and Tsabisis and the possibly mid-Ediacaran Bloeddriff cap carbonates in the Kalahari craton (Gaucher et al., 2005; Miller et al., 2009; Kaufman et al., 2009). However, $\delta^{13}C$ values for carbonates of the Jacoca Formation at the Capitão Farm are virtually all negative, in contrast with positive values observed in middle and upper sections of the Olhos D'Agua Formation in the eastern and western Vaza Barris domains (Fig. 16). On structural grounds, it is known that Jacoca Formation must be older than the Olhos D'Agua Formation (D'el Rey Silva, 1995, 1999). Both were weakly deformed during the Brasiliano cycle (628± Ma; Oliveira et al., 2006). The available youngest detrital-zircon age data for the Ribeiropolis (780 Ma) and Palestina Formation (653 Ma) suggest that the Jacoca Formation was likely deposited in the latest Cryogenian and that the Olhos D'Agua Formation is lowermost Ediacaran in age ("Marinoan" event). This is consistent with the U–Pb ages of 620 Ma for the youngest detrital zircon grains from the Frei Paulo Formation, which conformably overlies the Olhos D'Agua Formation.

Similarities of $^{87}Sr/^{86}Sr$ ratios of post-Sturtian and post-Marinoan carbonates led Babinski et al. (2007) to question the use of Sr-isotope stratigraphy to differentiate and correlate post-glacial carbonate successions.

2.3.6. Mercury stratigraphy

Mercury accumulation rate was found to be larger by a factor of three in Quaternary sediments deposited in a layer in Lagoa da Pata Basin, Upper Rio Negro, Brazilian Amazon, after the last glacial maximum than in a layer deposited before that (Santos et al., 2001). Thus, in regions where the geological background of mercury is negligible, mercury concentrations in sediments may be useful for paleoclimatological interpretation.

The Snowball Earth hypothesis assumes that mantle-derived CO_2 is transferred by volcanism to the atmosphere and its high concentration provokes meltout of ice and deposition of cap carbonates on top of glacial diamictites. Cataclysmic volcanoes have the potential to inject enough Hg to the atmosphere to change global and regional mercury cycles. For example, volcanic emissions of Hg to the atmosphere between 1980 and 2000 has totaled about 60 t yr^{-1} (Roos-Barraclough et al., 2002). Simultaneously, gold mining in South America, in particular in the Amazon Basin, was responsible for an annual emission varying between 50 and 100 t yr^{-1} (Lacerda, 2003). Therefore, it is true that the very surface of sediments and soils present Hg concentrations from both sources, plus an additional 40 t yr^{-1} derived from urban and industrial sources. Although Hg amalgamation has been in use in the Americas since 1540, with periods when annual emissions may have reached nearly 1000 t, nearly 50% to the atmosphere (Lacerda and Salomons, 1998), numerous results from sediment cores from bogs, lakes and the continental platform, agree that deposition prior to this period is close to the accepted natural background varying from <2 to 4.6 μg m^{-2} yr^{-1} (Lacerda et al., 1999; Santos et al., 2001; Barbosa et al., 2004; Lacerda and Ribeiro, 2004). Recent carbonate sediments along the Brazilian coast, for example, seldom show concentrations higher than a few μg^{-1}, at least during the entire Holocene. Therefore, the Hg stratigraphy of the Sergipano Belt was not affected by either gold mining emissions or even other anthropogenic sources occurring in the past 500 years.

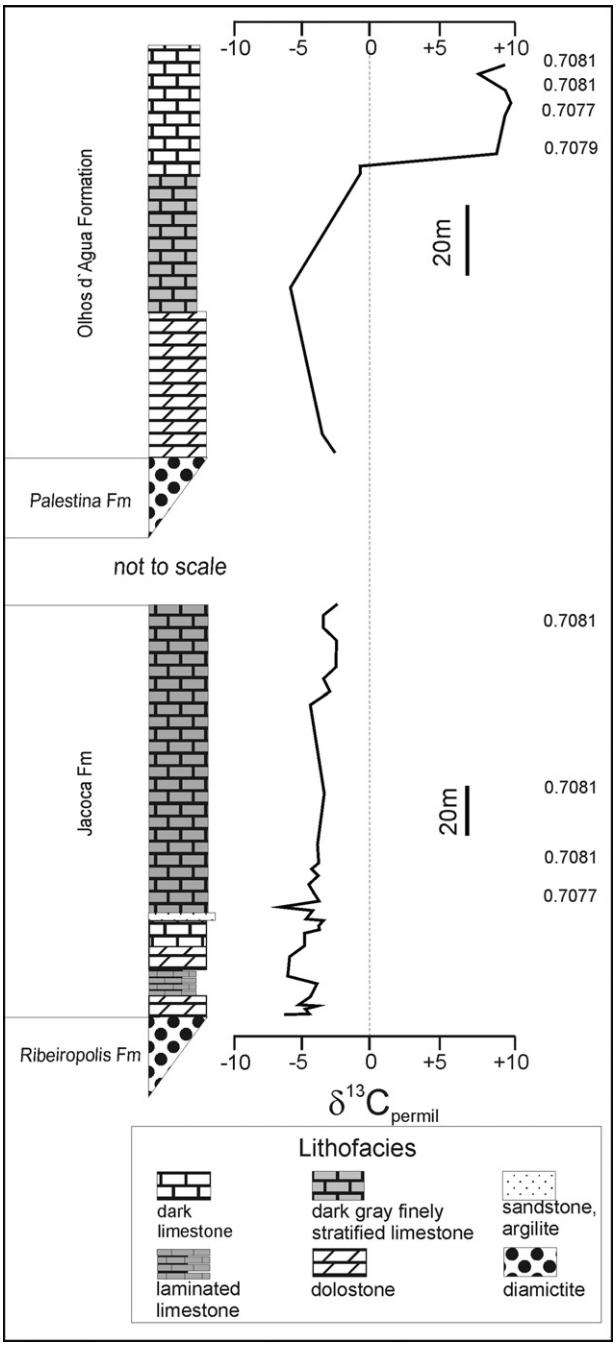

Fig. 16. Litho- and composite (^{13}C curve for carbonates of the Jacoca (Estancia-Miaba Group) and Olhos D'Agua Formations (Vaza Barris Group). The variation of Sr isotopes also shown in this composite section.

Table 5
Mercury contents (ng g^{-1}) of bulk carbonate samples from Acauã, Jacoca and OlhosÍÁgua Formations and mercury contents for Precambrian carbonate Formations of northeastern Brazil, Tertiary carbonates from Argentina and Chile and carbonatites from Brazil.

Acauã Formation, Bahia									Jacoca Formation, Sergipe			Olhos D'Agua Formation, Bahia		
São Gonçalo Farm			Patamuté village			Borracha Range			Capitão Farm			Capitão Range		
Sample	Height (m)	Hg	Sample	Height (m)	Hg	Sample	Height (m)	Hg	Sample	Height m)	Hg	Sample	Height (m)	Hg
EC-SG 01	0	22.9	PATA A	0.3	10.9	SB-06-2	0.6	4.83	JACS 01	0	0.94	SCAP-1A	0	9.21
EC-SG 02	0.5	11.0	PATA B	2.0	15.1	SB-06-4	3.0	4.27	JACS 02	0.3	1.88	SCAP-1B	10.0	1.86
EC-SG 03	0.5	10.9	PATA C	1.5	14.9	SB-06-5	1.5	6.01	JACS 03	0.3	1.04	SCAP-2	60.0	28.66
EC-SG 05	2.0	23.1	PATA 1	1.0	11.2	SB-06-6	1.0	0.00	JACS 04	0.3	1.80	SCAP-3	47.0	3.20
EC-SG 07	2.0	15.0	PATA 2	1.0	10.9	SB-06-12	14.0	0.00	JACS 05	0.3	2.58	SCAP-4	2.0	4.97
EC-SG 09	2.0	15.1	PATA 3	1.0	10,9	SB-06-13	3.0	0.00	JACS 06	0.3	3.75	SCAP-5	5.5	3.20
EC-SG 11	2.0	23.1	PATA 4	0.2	23.1	SB-06-14	5.0	0.00	JACS 07	0.1	1.80	SCAP-6	17.0	4.97
EC-SG 13	2.0	19.8	PATA 5	1.0	41.8	SB-06-15	5.0	0.00	JAC-CAP-1A	2.7	194.3	SCAP-7	5.0	15.82
EC-SG 15	2.0	26.2	PATA 7	0.5	10.8	SB-06-17	8.5	0.00	JAC-CAP-1B	0.6	*29.5*	SCAP-8	5.0	19.15
EC-SG 16	1.0	22.4	PATA 9	1.0	15.0	SB-06-20	11.0	1.92	JAC-CAP-1C	0.3	281.1	SCAP-9	7.0	28.88
			PATA 11	1.0	11.0	SB-06-28	38.5	4.04	JAC-CAP-1D	0.3	28.2	SCAP-10	2.0	82.64
			PATA 15	3.5	15.0	SB-06-38	35.0	2.26	JAC-CAP–1E	0.3	71.6			
			PATA 16	2.0	15.0	SB-06-40	14.5	4.06	JAC-CAP-01	0.3	24.8			
						SB-06-42	12.0	2.57	JAC-CAP-05	2.0	11.3			
									JAC-CAP-10	2.5	20.0			

Mesoproterozoic–Neoproterozoic Precambrian limestones (NE Brazil)						Tertiary limestones from Chile and Argentina						Brazilian carbonatites	
Macacos Farm		Pará		Flores		Topocalma		Punta Rocallosa		Yacoraite			
						Chile				Argentina			
Sample	Hg	Sample	Hg	Sample	Hg	Sample	Hg	Sample	Hg	Sample	Hg	Sample	Hg
MAC 01	0.68	Para 6-05	1.76	Malu 5	1.51	Topo 21	10.11	Proca 18	23.01	Yacor 5	1.51	Jacu	1.3
MAC 02	4.3	Para 6-08	1.85	Malu 10	5.81	Topo 9	7.95	Proca 30	72.80	Yacor 16	1.51	Anitapolis	16.7
MAC 07	1.57	Para 6-09	1.78	Malu 21	1.51					Yacor 17	1.51	Lages	1.75
MAC 19	0.93	Para 6-15	0.90	Flor 5	1.51					Yacor 23	3.66	Araxá	2.34
		Para 6-16	0.82	Flor 39	3.66							Catalão	3.24

Roos-Barraclough et al. (2002) found evidence of increasing Hg deposition in lake sediment cores from the Swiss Jura Mountains corresponding to known volcanic eruptions. Thus, volcanism may have allowed also for higher concentrations of Hg in cap carbonates after ice melting.

To our knowledge, no databank available for mercury in sedimentary carbonates is available. As a preliminary survey, five samples of Precambrian carbonates (Meso-Neoproterozoic transition, São Caetano complex, state of Pernambuco, northeastern Brazil), Tertiary limestones from Topocalma (Chile) and Punta Rocallosa (Chilean Patagonia), and Cretaceous–Tertiary Yacoraite limestones (Argentina) were analyzed. There is no clear indication that these carbonates were deposited concurrently to volcanic activity, except at Punta Rocallosa (Table 5). Precambrian carbonates and Mesozoic to Tertiary carbonates of the Yacoraite Formation yielded values between 1.5 and 6 ng g^{-1} of mercury, while carbonates from Topocalma exhibited values of 8 and 10 ng g^{-1}. However, two carbonate samples from Punta Rocallosa, yielded values of 23 and 73 ng g^{-1}. Carbonatites from five localities in Brazil were also analyzed yielding always mercury contents below 3 ng g^{-1} except for a sample from the carbonatite of Anitapolis which has shown a value of 16 ng g^{-1}. In conclusion, in light of these new data, we conclude that Hg contents in sedimentary and igneous carbonates are usually below 3 ng g^{-1}, except when concomitant volcanism caused an uprise of atmospheric Hg as at Punta Rocallosa that supposedly has been deposited near the Cretaceous–Tertiary boundary.

A Hg survey with carbonate samples from the Acauã and Jacoca Formations (53 samples) and Olhos D'Agua Formation (11 samples)

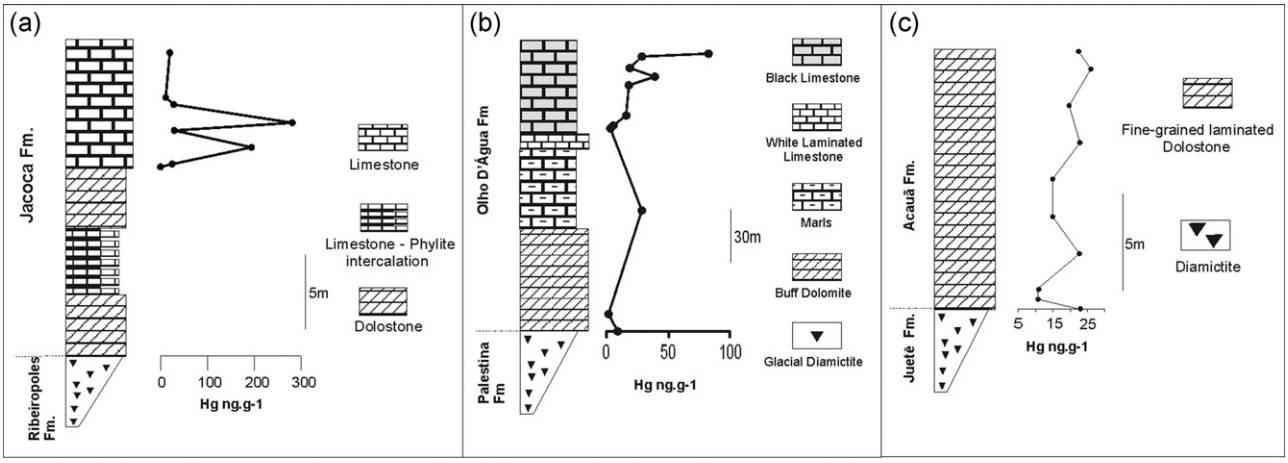

Fig. 17. Mercury stratigraphy for carbonates of (a) Jacoca Formation at Capitão Farm, Sergipe; (b) Olhos D'Agua Formation at the Capitão Range and (c) Acauã Formation at São Gonçalo Farm, Bahia.

was carried out, aiming to use Hg concentrations as a proxy of volcanism intensity and CO_2 buildup. In this attempt, only localities where carbonates were seen in sharp – but not erosional – contact with basal diamictites and that show $\delta^{13}C$ values around −5‰ have been analyzed for Hg contents. In this way, only carbonates deposited at the earliest stages of the aftermath of glacial events were analyzed.

At Capitão Farm (Fig. 17a), near the Vaza Barris River, two carbonate samples of Jacoca Formation about 15 m from the base of the section (limestone-pelite intercalation) showed mercury contents of 281 and 194 ng g^{-1}, higher by a factor of 10, if compared to the rest of this profile (average 20 ng g^{-1}). The association of higher contents of mercury in carbonates finely inter-layered with terrigenous sediments suggests that higher mercury atmospheric deposition, originated from volcanism, resulted in higher leaching from land surface accumulating along argillaceous carbonates, similarly to the processes described in the Swiss Jura Mountains for quaternary sediments (Roos-Barraclough et al., 2002).

At Capitão Range (Fig. 17b), carbonates of the Olhos D'Agua Formation show a total variation from <3 to 83 ng g^{-1} with a strong increase towards the top (organic-rich, dark carbonates show higher values). In this section, the basal part shows a distinctively different behavior compared with the upper part, which displays much higher $\delta^{13}C$ values.

Presence of organic matter seems to be the main Hg immobilizer in sedimentary rocks, decreasing substantially it's leaching after deposition. In some lakes with sedimentation enriched in organic matter, Hg contents may reach values as high as 600 ng g^{-1} as at Carajás, for example, in northern Brazil (Lacerda et al., 1999).

At São the Gonçalo Farm section, where a sharp contact between diamictite and cap dolostone of the Acauã Formation is observed, a single dolostone sample few centimeters from the contact yielded a value of 30 ng g^{-1} (Fig. 17c). From this point, the stratigraphic curve shows a gradual increase upsection from 11 to 26 ng g^{-1} (average 19 ± 5). At Serra da Borracha (not shown), a rhythmic variation of Hg content was observed (total variation from <3 to 20 ng g^{-1}), while at Patamuté (not shown), values are around 11 ng g^{-1} with an increase to 41 ng g^{-1} where gray marl grades into calcareous phyllite, at about 8 m from the basal contact.

3. Discussion and conclusions

In the light of the C-isotope data presented here, (^{13}C values for two of the cap carbonates under consideration are all negative, even in thick sections (e.g. 165 m of the Acauã Formation in the Serra da Borracha and 80 m for the Jacoca Formation in the Capitão Farm). The third cap carbonate (Olhos D'Agua Formation) also shows this unusual behavior and negative values have been observed for about 100 m (section near the road Simão Dias-Pinhão villages), shifting to positive values up section (+8 to +10‰).

Despite of the large effort made to date Neoproterozoic glaciations (Hoffmann et al., 2004; Fanning and Link, 2004; Zhou et al., 2004; Calver et al., 2004) this subject is still a matter of strong debate. Therefore, any compiled temporal (^{13}C secular variation curve becomes a mobile target and its use, perhaps, leads to erroneous assumptions.

Current detrital zircon ages for the Ribeiropolis diamictite below the Jacoca Formation, and for the Palestina diamictites below the Olhos D'Agua Formation suggest these carbonates have been deposited, respectively, after 780 Ma and after 653 Ma. Furthermore, both were deformed and metamorphosed during the Brasiliano orogeny (628 ± 12 Ma; Oliveira et al., 2006). This strongly suggests that the Olhos D'Agua Formation was deposited in the lowermost Ediacaran (*ca*. 635 Ma "Marinoan") and that the Palestina Formation is probably a correlate of the Ghaub glacials in Namibia. One problem with this scheme is the magnitude of the positive (^{13}C excursion in all of the studied sections of the upper Olhos D'Agua Formation, unusually high (up to +9‰ PDB) for Ediacaran carbonates. Given the steep carbon isotope gradients of Neoproterozoic oceans (Calver, 2000; Shen et al., 2005), this may be the result of a shallower setting and/or a semi-restricted basin. An extended negative (^{13}C excursion followed by an abrupt positive crossover is just what has been described for the Ghaub and Maieberg formations in Namibia (see Fig. 10 in Halverson et al., 2005). There, (^{13}C also reaches +9‰ in the upper Elandshoek and lower Hüttenberg formations.

The Jacoca and Acauã formations are typical cap carbonates, with tubestone stromatolites, megaripples/hummocky and typical "buff" dolostone. The underlying Juetê and Ribeirópolis diamictites are very similar to each other and quite different from the Palestina Formation diamictite. Moreover, both Jacoca and Acauã begin with shallow-water dolostone, and pass into a deepening-upward carbonate succession. The Olhos D'Agua Formation, in turn, was mostly deposited in deeper water, although shallow-water facies with stromatolites and buff dolostones have been also observed. Finally, the Jacoca and Acauã formations exhibit nearly identical carbon isotope curves, which are distinctively different from curve obtained for the Olhos D'Agua Formation.

It is difficult to assign an age to the Jacoca Formation. Its $^{87}Sr/^{86}Sr$ values may have been partially reset, as usual for many successions. It was probably deposited in the Cryogenian, but its precise age cannot be inferred from our current data. As for the Acauã Formation, one avails even less firm evidence to assign it an age. These two formations are probably correlative and the Acauã Formation may represent the shallower facies on the São Francisco Craton, in contrast with the deeper water deposits of the Jacoca Formation. If $^{87}Sr/^{86}Sr$ values for the Jacoca or Acauã formations have been reset, then nothing precludes this correlation. Carbon isotopes are much more robust to secondary alteration and support a correlation of the Jacoca and Acauã formations. The age of these units is probably anywhere between 740 and 650 Ma. Fossil record data in combination with the available isotope data will help solving this issue.

Available Ca-isotope data points to a Cryogenian age for the Jacoca Formation and a lowermost Ediacaran age for the Acauã Formation (Silva Tamayo et al., 2010).

High Hg concentrations in carbonates and carbonatic phyllites of the Jacoca Formation may have resulted from volcanism that followed a snowball event. Mercury chemostratigraphy could be potentially used as a tracer for glacial events and to estimate the buildup of volcanic gases (including CO_2) during glaciation.

Acknowledgements

We want to express our gratitude to Teodomiro Mendes Filho for logistic support during our field work at the Borracha and Canabrava Ranges, in northern Bahia. We are grateful to the National Council for Scientific and Technological Development for financial support (projects n. 472506/2003-0, 490180/2003-5, 490349/2004-8 and 475657/2006-3) as well as to FACEPE (project n. APQ 0727-1.07/08). Thanks are also due to W.R. Van Schmus for unpublished zircon age data. This is the contribution n. 252 of the Nucleus for Geochemical Studies-Stable Isotope Laboratory (NEG-LABISE), Dept. of Geology, Federal University of Pernambuco, Brazil.

References

Allard, G.O., Hurst, V.J., 1969. Brazil-Gabon geological link supports continental drift. Science 163, 528–532.

Babinski, M., Vieira, L.C., Trindade, R.I.F., 2007. Direct dating of the Sete Lagoas cap carbonate (Bambuí Group, Brazil) and implications for the Neoproterozoic glacial events. Terra Nova 19, 401–406.

Barbosa, J.A., Cordeiro,,. Silva, R.C., Turcq, E.V., Gomes, B., Santos, P.R.S., Sifeddine, G.M., Albuquerque, A., Lacerda, A.L.S., Hausladen, L.D., Tims, P.A., Levchenco, S.G., Fifield LK, V.A., 2004. ^{14}C-MAS as a tool for the investigation of mercury deposition at a remote Amazon location. Nucl. Instrum. Methods Phys. Res. B 223–224, 528–534.

Bowring, S., Myrow, P., Landing, E., Ramezani, I., Grotzinger, J., 2003. Geochronological constraints on Terminal Neoproterozoic events and the rise of metazoans. Geophysical Research Abstracts 5, 13219.

Brito Neves, B.B., Sial, A.N., Albuquerque, J.P.T., 1977. Vergência centrífiga residual no Sistema de Dobramentos Sergipano. Revista Brasileira de Geociências 7, 102–114.

Calver, C., 2000. Isotope stratigraphy of the Ediacaran (Neoproterozoic III) of the Adelaide Rift Complex, Australia, and the overprint of water column stratification. Precambrian Res. 100, 121–150.

Calver, R.C., Black, L.P., Everard, J.L., Seymour, D.B., 2004. U-Pb zircon age constraints on late Neoproterozoic glaciation in Tasmania. Geology 32, 893–896.

Chumakov, N.M., 2009. Neoproterozoic glacial events in Eurasia. In: Gaucher, C., Sial, A.N., Halverson, G.P., Frimmel, H. (Eds.), Neoproterozoic-Cambrian Tectonics, Global Change and Evolution: A Focus on Southwestern Gondwana. Developments in Precambrian Geology, 16. Elsevier, pp. 389–403.

Condon, D., Zhu, M., Bowring, S., Jin, Y., Wang, W., Yang, A., 2005. From the Marinoan glaciation to the oldest bilaterians: U–Pb ages from the Doushantuo Formation China. Science 308, 95–98.

Cordani, U.G., 1973. Evolução geológica Precambriana da faixa costeira do Brasil antre Salvador e Vitoria. Tese de Livre Docência, Instituto de Geociências, Universidade de São Paulo, São Paulo, 98 p.

Craig, H., 1957. Isotopic standards of carbon and oxygen and correction factors for mass-spectrometric analysis of carbon dioxide. Geochim. Cosmochim. Acta 12, 133–149.

Davison, I., Santos, R.A., 1989. Tectonic evolution of the Sergipano Fold, NE Brazil, during the Brasiliano Orogeny. Precambrian Res. 45, 319–342.

D'el Rey Silva, L.J.H., 1995. The evolution of basement gneiss domes of the Sergipano fold belt (NE Brazil) and its importance for the analysis of Proterozoic basins. J. S. Am. Earth Sci. 8, 325–340.

D'el Rey Silva, L.J.H., 1999. Basin in-filling in the southern-central part of the Sergipano Belt (NE Brazil) and implications for the evolution of Pan-African/Brasiliano cratons and Neoproterozoic sedimentary cover. J. S. Am. Earth Sci. 4–5, 1–18.

Derry, L.A., Kaufman, A.J., Jacobsen, S.B., 1992. Sedimentary cycling and environmental, change in the Late Proterozoic: evidence from stable and radiogenic isotopes. Geochimica et Cosmochimica Acta 59, 1317–1329.

Fanning, M., 2006. Constraints on the timing of the Sturtian Glaciation from Southern Australia; ie for the true Sturtian. Geol. Soc. Am. Abstr. Programs 38, 115.

Fanning, C.M., Link, P.K., 2004. U–Pb SRIMP ages of Neoproterozoic (Sturtian) glaciogenic Pocatello Formation, southeastern Idaho. Geology 32, 881–884.

Fölling, P.G., Frimmel, H.E., 2002. Chemostratigraphic correlation of carbonate succesions in the Gariep and Saldania Belts, Namibia and South Africa. Basin Res. 13, 1–37.

Frimmel, H.E., Klötzli, U., Siegfried, P., 1996. New Pb-Pb single zircon age constraints on the timing of Neoproterozoic glaciation and continental break-up in Namibia. J. Geol. 104, 459–469.

Gaucher, C., Sial, A.N., Blanco, G., Sprechmann, P., 2004. Chemostratigraphy of the lower Arroyo del Soldado Group (Vendian, Uruguay) and palaeoclimatic implications. Gondwana Res. 7, 715–730.

Gaucher, C., Frimmel, H.E., Germs, G.J.B., 2005. Organic-walled microfossils and biostratigraphy of the upper Port Nolloth Group (Namibia): implications for the latest Neoproterozoic glaciations. Geol. Mag. 142 (5), 539–559.

Gaucher, C., Sial, A.N., Poiré, D., Gómez-Peral, L., Ferreira, V.P., Pimentel, M.M., 2009. Chemostratigraphy. Neoproterozoic-Cambrian evolution of the Río de la Plata Palaeocontinent. In: Gaucher, C., Sial, A.N., Halverson, G.P., Frimmel, H. (Eds.), Neoproterozoic-Cambrian Tectonics, Global Change and Evolution: A Focus on Southwestern Gondwana. Developments in Precambrian Geology, 16. Elsevier, pp. 115–122.

Germs, G.J.B., 1995. The Neoproterozoic of southwestern Africa, with emphasis on platform stratigraphy and paleontology. Precambrian Research 73, 1376–2151.

Germs, G.J.B., Miller, R.Mc.G., Frimmel, H.E., Gaucher, C., 2009. Syn- to late-orogenic sedimentary basins of southwestern Africa. Neoproterozoic to Early Palaeozoic evolution of southwestern Africa. In: Gaucher, C., Sial, A.N., Halverson, G.P., Frimmel, H. (Eds.), Neoproterozoic-Cambrian Tectonics, Global Change and Evolution: A Focus on Southwestern Gondwana. Developments in Precambrian Geology, 16. Elsevier, pp. 183–203.

Halverson, G.P., Hoffman, P.F., Schrag, D.P., Maloof, A.C., Rice, A.H.N., 2005. Toward a Neoproterozoic composite composite carbon-isotope record. Geol. Soc. Am. Bull. 117, 1181–1207.

Halverson, G.P., Dudas, F.O., Maloof, A.C., Bowring, S.A., 2007. Evolution of the $^{87}Sr/^{86}Sr$ composition of the Neoproterozoic seawater. Paleogeog. Paleoclim. Paleoecol. 526, 103–129.

Halverson, G.P., Hurtgen, M.T., Porter, S.M., Collins, A.S., 2009. Neoproterozoic-Cambrian biogeochemical evolution. In: Gaucher, C., Sial, A.N., Halverson, G.P., Frimmel, H. (Eds.), Neoproterozoic-Cambrian Tectonics, Global Change and Evolution: A Focus on Southwestern Gondwana. Developments in Precambrian Geology, 16. Elsevier, pp. 351–365.

Hoffman, P.F., Kaufman, A.J., Halverson, G.P., 1998. Comings and goings of global glaciations on a Neoproterozoic tropical platform in Namibia. GSA Today 8 (5), 129.

Hoffman, P.F., Hawkins, D.P., Isachsen, C.E., Bowring, S.A., 1996. Precise U-Pb zircon ages for early Damaran magmatism in the Summas Mountains and Welwitschia inlier, northern Damara belt, Namibia. Commun. Geol. Surv. Namibia 11, 47–52.

Hoffman, P.F., Schrag, D.P., 2002. The snowball Earth hypothesis: testing the limits of global change. Terra Nova 14, 129–155.

Hoffman, P.F., Li, Z.-X., 2009. A palaeogeographic context for Neoproterozoic glaciation. Palaeogeogra. Palaeoclimatol. Palaeoecol. 277, 158–172.

Hoffmann, K.H., Condon, D.J., Bowring, S.A., Crowley, J.L., 2004. U-Pb zircon date from the Neopro-terozoic Ghaub Formation Namibia: constraints on Ma-rinoan glaciation. Geology 32 (9), 817–820.

Humphrey, F.L. and Allard, G.O., 1969. Geologia da área do domo de Itabaiana (Sergipe) e sua relação com a geologia de Propriá: um elemento recém-reconhecido no escudo brasileiro. Petrobras, Centro de Pesquisa e Desenvolvimento (CENPES), Rio de Janeiro, Brazil, 159p. (in Portuguese and English).

Jacobsen, S.B., Kaufman, A.J., 1999. The Sr, C and O isotopic evolution of Neoproterozoic seawater. Chem. Geol. 161, 37–57.

Jordan, H., 1973. Mapa geológico da Região Barro Vermelho-Patamuté 1:100.000. SUDENE-DRN, Divisão de Geologia, Recife, Brazil.

Kaufman, A.J., Knoll, A.H., 1995. Neoproterozoic variations in the C-isotopic composition of seawater: stratigraphic and biogeochemical implications. Precambrian Res. 73, 27–49.

Kaufman, A.J., Jacobsen, S.B., Knoll, A.H., 1993. The Vendian record of Sr and isotopic variations in seawater: implications for tectonics and paleoclimatic. Earth Planet. Sci. Lett. 120, 409–430.

Kaufman, A.J., Knoll, A.H., Narbonne, G.M., 1997. Isotopes, ice ages, and terminal Proterozoic earth history. Proc. Natl. Acad. Sci. USA 94, 6600–6605.

Kaufman, A.J., Sial, A.N., Frimmel, H.E., Misi, A., 2009. Neoproterozoic to Cambrian Palaeoclimatic Events in Southwestern Gondwana. In: Gaucher, C., Sial, A.N., Halverson, G.P., Frimmel, H. (Eds.), Neoproterozoic-Cambrian Tectonics, Global Change and Evolution: A Focus on Southwestern Gondwana. Developments in Precambrian Geology, 16. Elsevier, pp. 369–388.

Kennedy, M.J., 1996. Stratigraphy, sedimentology, and isotopic geochemistry of Australian cap dolostones: deglaciation, d13C excursions, and carbonate precipitation. Journal of Sedimentary Research 66, 1050–1064.

Kha, L.C., Sherman, A.G., Narbonne, G.M., Knoll, A.H., Kaufman, A.J., 1999. $\delta^{13}C$ stratigraphy of the Proterozoic Bylot Supergroup, Baffin Island, Canada: implications for regional lithostratigraphic correlations. Can. J. Earth Sci. 36, 313–332.

Knoll, A.H., Kaufman, A.J., Semikhatov, M.A., 1995. The carbon isotopic composition of Proterozoic carbonates: Riphean successions from northwestern Siberia (Anabar Massif, Turukhansk Uplift). Am. J. Sci. 295, 823–850.

Lacerda, L.D., 2003. Updating global mercury emissions from small-scale gold mining and assessing its environmental impacts. Environ. Geol. 43, 308–314.

Lacerda, L.D., Ribeiro, M.G., 2004. Changes in lead and mercury loads to southeastern Brazil due to industrial emissions during the 20th century. J. Braz. Chem. Soc. 15, 931–937.

Lacerda, L.D., Salomons, W., 1998. Mercury Contamination from Gold and Silver Mining. A Chemical Time Bomb. Springer–Verlag, Berlin, 146 p.

Lacerda, L.D., Ribeiro, M.G., Cordeiro, R.C., Siffedine, A., Turcq, B., 1999. Atmospheric Mercury deposition over Brazil during the past 30,000 years. Ciencia e Cultura. J. Braz. Assoc. Adv. Sci. 15, 363–371.

Miller, R.Mc.G., Frimmel, H.E., Halverson, G.P., 2009. Passive continental margin evolution. Neoproterozoic to Early Palaeozoic evolution of Southwestern Africa. In: Gaucher, C., Sial, A.N., Halverson, G.P., Frimmel, H. (Eds.), Neoproterozoic-Cambrian Tectonics, Global Change and Evolution: A Focus on Southwestern Gondwana. Developments in Precambrian Geology, 16. Elsevier, pp. 161–181.

Nogueira, A.C.R., Riccomini, C., Sial, A.N., Moura, C.A.V., Fairchild, T.R., 2003. Soft-sediment deformation at the Neoproterozoic Puga cap carbonate (southwestern Amazon Craton, Brazil): confirmation of rapid icehouse to greenhouse transition in snowball Earth. Geology 31, 516–613.

Oliveira, E.P., 2008. Evolução geológica da Faixa Sergipana, limite sul da Província Borborema. Workshop sobre a Geologia do Precambriano da Província Borborema. Campinas, São Paulo, pp. 14–15.

Oliveira, E.P., Toteu, S.F., Araújo, M.J., Cravalho, M.J., Nascimento, R.S., Bueno, J.F., McNaughton, N., Basilici, G., 2006. Geologic correlation between the Neoproterozoic Sergipano belt (NE Brazil) and the Yaoundé belt (Cameroon, Africa). J. Afr. Earth Sci. 44, 470–478.

Ripperdan, R.L., Magaritz, M., Nicoll, R.S., Shergold, J.H., 1992. Simultaneous changes in carbon, sea level, and conodont biozones within Cambrian–Ordovician boundary interval at Black Mountain, Australia. Geology 20, 1039–1042.

Roos-Barraclough, F., Martinez-Cortizas, A., Garcia-Rodeja, E., Shotyk, W., 2002. A 14500 year record of the accumulation of atmospheric mercury in peat: volcanic signals, anthropogenic influences and a correlation to bromine accumulation. Earth Planet. Sci. Lett. 202, 435–451.

Santos, R.A., Souza, J.D., 1988. Programa Levantamentos Geológicos Básicos do Brasil; carta metalogenética/previsional, escala 1:100,000 (Folha SC.24-X-C-VI Piranhas). DNPM/CPRM, 154 p.

Santos, R.A., Martins, A.A.M., Neves, J.P., Leal, R.A., 1998. Geologia e Recursos Minerais do Estado de Sergipe. CPRM, Codise, 107.

Santos, G.M., Cordeiro, R.C., Silva Filho, E.V., Turcq, B., Lacerda, L.D., Fifield, L.K., Gomes, P.R.S., Hausçaden, P.A., Sifeddine, A., Albuquerque, A.L.S., 2001. Chronology of the atmospheric mercury in Lagoa da Pata Basin, Upper Rio Negro of Brazilian Amazon. Radiocarbon 43, 801–808.

Shen, Y., Zhangb, T., Chub, X., 2005. C-isotope stratification in a post-glacial ocean. Precambrian Res. 137, 243–251.
Sial, A.N., Dardenne, M.A., Misi, A., Pedreira, A.J., Ferreira, V.P., Silva Filho, M.A.C., Gaucher, C., Uhlein, A., Pedrosa-Soares, A.C., Santos, R.V., Egydio-Silva, M., Babinski, M., Alvarenga, C.J., Fairchild, T.R., Pimentel, M.M., 2009. The São Francisco paleocontinent. In: Gaucher, C., Sial, A.N., Halverson, G.P., Frimmel, H. (Eds.), Neoproterozoic-Cambrian Tectonics, Global Change and Evolution: A Focus on Southwestern Gondwana. Developments in Precambrian Geology, 16. Elsevier, pp. 31–69.
Sial, A.N., Ferreira, V.P., Almeida, A.R., Romano, A.W., Parente, C.V., Costa, M.L., Santos, V.H., 2000. Carbon isotope fluctuations in Precambrian carbonate sequences of several localities in Brazil. Anais Academia Brasileira de Ciências 72, 539–558.
Sial, A.N., Ferreira, V.P., Silva Filho, M.A., Gaucher, C., Soares, D.R., Silva Filho, E.V., Pimentel, M.M., Lacerda, L.D., Gantois, G., 2006. Chemostratigraphy of two Neoproterozoic cap carbonates of the Sergipano belt (northeastern Brazil). Short Papers, V South American Symposium on Isotope Geology. Punta del Este, Uruguay, pp. 314–317.
Silva Filho, M.A., 1998. Arco vulcânico Canindé-Marancó e a Faixa Sul-Alagoana: sequências orogênicas mesoproterozoicas. IX Congresso Brasileiro de Geologia, Belo Horizonte, Minas Gerais, p. 16.
Silva Filho, A.F., Acioly, A.C.A., Torres, H.H.F., Araújo, R.V., 2003. O complexo Jaramataia no contexto do Sistema Sergipano. Revista de Geologia 16, 99–110.
Silva Filho, M.A., Brito Neves, B.B., 1979. O sistema de dobramentos Sergipano no Nordeste da Bahia. Geologia Recursos Miner. Estado Bahia, Textos Básicos 1, pp. 203–217.
Silva Filho, M.A., Torres, H.H.F., 2002. A new interpretation on the Sergipano belt Domain. Anais da Academia Brasileira de Ciencias 74, 556–557.
Silva Tamayo, J.C., Nägler, T., Villa, I.M., Kyser, K., Vieira, L.C., Sial, A.N., Narbonne, G.M., James, N.P. 2010. Global Ca isotope variations in Post-Sturtian carbonate successions. Terra Nova, June, 188–194.
Trompette, R., 1994. Geology of Western Gondwana (2000-500 Ma). A.A. Balkema, Rotterdam (350 p).
Xu, B., Xiao, S., Zou, H., Chen, Y., Li, Z.X., Song, B., Liu, D., Zhou, C., Yuan, X., 2009. SHRIMP zircon U-Pb age constraints on Neoproterozoic Quruqtagh diamictites in NW China. Precambrian Res. 168, 247–258.
Zhou, C., Tucker, R., Xiao, Peng, Z., Yuan, X., Chen, Z., 2004. New constraints on the ages of Neoproterozoic glaciations in south China. Geology 32, 437–440.